A Tsunami Forecast Model for Myrtle Beach, South Carolina

Hongqiang Zhou[1,2] and David Burwell[1,2]

1. NOAA Center for Tsunami Research, Pacific Marine Environmental Laboratory, Seattle, WA
2. Joint Institute for the Study of the Atmosphere and Ocean, Seattle, WA

Abstract   This report documents the development, validation and stability testing of a tsunami forecast model for Myrtle Beach, South Carolina. The model is to be integrated into NOAA's Short-term Inundation Forecast of Tsunamis system. In the forecast model, propagation and inundation of water waves in a tsunami event are simulated in three telescoped nested grids in real time. The innermost grid has a resolution of $3''$ (~ 93 m) and covers the population and economic center of the Myrtle Beach. The model requires less than 7 minutes of CPU time to accomplish a 12-hour simulation. Accuracy and stability of the forecast model is proved in a series of synthetic tsunami scenarios.

Contents

List of Figures

3

List of Tables

1 Background and Objectives

The National Oceanic and Atmospheric Administration (NOAA) Center for Tsunami Research (NCTR) at the NOAA Pacific Marine Environmental Laboratory has developed a tsunami forecasting capability for operational use by NOAA's two Tsunami Warning Centers located in Hawaii and Alaska (Titov et al., 2005). The system, termed Short-term Inundation Forecast of Tsunamis (SIFT), is designed to efficiently provide basin-wide warning of approaching tsunami waves accurately and quickly. The SIFT system combines real-time tsunami event data with numerical models to produce estimates of tsunami wave arrival time and amplitudes at coastal communities of interest. This system integrates several key components: deep-ocean observations of tsunamis in real time, a basin-wide pre-computed propagation database of water level and flow velocities based on potential seismic unit sources, an inversion algorithm to refine the tsunami source based on deep-ocean observations during an event, and inundation forecast models run in real time and at high resolutions for selected coastal communities.

In developing the tsunami forecast system, we plan to cover most of the tsunami-threatened communities of the U.S. states and territories including the city of Myrtle Beach, South Carolina. Myrtle Beach is located on the lowlands along the east coast of South Carolina and faces the Atlantic Ocean (Long Bay, which is actually a bite not a "bay"). Parallel to the coast of the Long Bay runs the intracoastal waterway, which was built in the 19th century and is still serving the east and gulf coasts. Thanks to its warm subtropical climate and extensive beaches, Myrtle Beach is one of the major tourism centers of the U.S., visited by approximately 14 million tourists per year. According to he 2010 census, the city has a population of 27109 and an area of 60.4 km^2 (U.S. Census Bureau, 2013).

Although there is no record of historical tsunami hazards in this area, Myrtle Beach may be subject to tsunamis generated by earthquakes in the Atlantic basin, especially the eastern edge of the Caribbean Plate and the eastern edge of the Scotia Plate. Besides earthquakes, submarine and subaerial landslides may also trigger tsunamis and threat the U.S. east coast cities including Myrtle Beach (e.g., Driscol et al., 2000; Ten Brink et al., 2008; Løvholt et al., 2008; Zhou et al., 2011). In this study, we develop a tsunami forecast model for the city of Myrtle Beach. This model is to be integrated into the SIFT system as a part of NOAA's effort to provide a nation-wide tsunami forecast capability.

2 Forecast Methodology

A forecast model is designed to provide a quick and accurate estimate on tsunami arrival time, wave heights, and inundated areas during a tsunami event. In the SIFT system, all the models are designed and tested to perform under stringent time constraints, given that time is generally the single limiting factor in saving lives and properties. The core of a forecast model is a numerical model, which simulates the nearshore wave propagation and coastal inundation in real time with a numerical code, Method of Splitting Tsunami (MOST). MOST solves the shallow water equations through a finite difference scheme. The code has been extensively validated against laboratory experiments (Synolakis et al., 2008), as well as historical tsunami events (Wei et al., 2008; Tang et al., 2008). In a forecast model, simulations are conducted in three telescoped nested grids at successively increased

resolutions. The innermost grid covers the population and economic center of a community of interest. The grids are constructed based on the digital elevation models (DEMs) developed by the National Geophysical Data Center (NGDC) and NCTR. Readers are referred to Titov and González (1997) for the technical aspects of forecast model development, validation and stability testing, and Tang et al. (2009) for the details of forecast methodology.

Basin-scale computations of tsunami propagation can be very time-consuming and is almost impossible in real-time forecasts at current stage. Instead of real-time simulation, propagation of water waves in the ocean basins due to a "unit earthquake source" is precomputed and the time-series of water surface elevations and water velocities are stored in the propagation database as a "unit tsunami source function". A unit earthquake source has a measurement of 100×50 km^2 in area and a slip value of 1 m, equivalent to the moment magnitude (Mw) of 7.5 (Gica et al., 2008). All subduction zones in the ocean basins are split entirely into numerous unit earthquake sources. Given that the tsunami evolution in deep ocean is a linear process, a tsunami scenario can be accurately represented through the linear combination of related source functions. During a tsunami event, as the waves propagate across the ocean and successively reach the DART ("Deep-Ocean Assessment and Reporting of Tsunamis") observation sites, measured sea level is ingested into the tsunami forecast application in near real time and incorporated into an inversion algorithm to produce an improved estimate of the tsunami source (Percival et al., 2009, 2011).

Nonlinear effects become significant when the waves approach the near shore in shallower water. This process is computed in real time in the tsunami forecast model. The model consists of three nested grids, named A, B, and C-grids with successively increased resolutions. The outermost A-grid provides a smooth transition from the propagation database to the nearshore real-time simulation. The A-grid covers a large domain with offshore boundaries extended into deep ocean. During a tsunami event, synthetic boundary conditions are obtained along the open boundaries of A-grid through the linear combination of tsunami source functions. The population and economic center of the target community is covered by the C-grid at a high resolution in order to represent the details of bathymetry and topography, as well as to mitigate numerical errors in the numerical model.

The accuracy and efficiency of tsunami forecast models in the Pacific region currently implemented in the forecast system have been validated in recent tsunami events (Titov et al., 2005; Titov, 2009; Tang et al., 2008; Wei et al., 2008).

3   Model Development

The accuracy of tsunami forecast largely relies on the accuracy of bathymetry and topography. The bathymetry and topography used in the development of the forecast model for Myrtle Beach are based on a DEM provided by NGDC and we consider it to be an adequate representation of the local topography and bathymetry. As new DEMs become available, forecast models will be updated and report updates will be posted at "`http://nctr.pmel.noaa.gov/forecast_reports`".

In developing a forecast model, a high-resolution "reference" model is first developed. The reference model is considered to best represent the processes in a tsunami event, without losing any accuracy due to resolution or numerical errors. This model may consume a very long CPU time and therefore is not efficient for forecast purpose. An "optimized" model

is constructed by downgrading the resolutions and reducing the domain coverage of the reference model grids. The purpose of this optimization is to reduce the CPU time to an operationally specified period, which is 10 minutes or less for a 4-hour simulation. This operationally developed model is referred to as the "optimized tsunami forecast model", or simply the "forecast model". In the development of a forecast model, the computational results are carefully compared between the reference and forecast models to make sure that due accuracy is maintained in the latter.

3.1 Forecast area

Figure 1 shows the location of Myrtle Beach on "Google Maps". The city domain is separated from the mainland by a waterway on the northwest. As a result, its development has been constrained within a small distance from the Atlantic coast. Due to strong erosion along the coast, the waterfront of Myrtle Beach experiences a retreat up to 30 cm per year. To compensate this loss, the state refills them every seven years or so with sediment dredged from sea bottom (Storrs, 2009). Because of these factors, as well as that the terrain is very flat and low-lying (most of it is less than 10 m above sea level, see Figure 2), Myrtle Beach is vulnerable to coastal flooding hazards due to tsunamis and storm surges.

3.2 Grid setup

The computational grids have the same domain coverage in both reference and forecast models, but different resolutions. Domain coverages of these grids are presented in Figure 2, and their parameters are tabulated in Table 1. The A-grids in both models cover an area extending from dry land into deep ocean, serving a smooth transition from the propagation database to real-time simulations with the nonlinear numerical model. In the reference model, this grid has a resolution of $36''$, while it is $72''$ in the forecast model. High-resolution topography is neglected in A-grids. Considering that wave runup is not computed in A- and B-grids, neglecting topography in these grids does not affect the numerical results. The B-grids provide an interim step in the simulations, and have the same resolution of $9''$ in both models. Tsunami inundation in Myrtle Beach area is computed in C-grids at resolutions of $2''$ and $3''$ in the reference and forecast models, respectively. There is a tide gage installed at Springmaid Pier in Myrtle Beach ($33°39.3'$N, $78°55.1'$W), where mean high water depth is 5.25 m and mean range of tide is 1.53 m. The tide gage currently in operation was installed on August 23, 1977.

In Figure 2, we also plot the contours of water depth in A-grids. The U.S. Atlantic coast, including that in Myrtle Beach area, is confronted with a continental shelf, which extends nearly 100 km into the Atlantic basin and has a water depth mostly less than 50 m. When long waves propagate into shallow water over the continental shelf, wave speeds decrease rapidly and a lot of wave energy is dissipated due to bottom friction. This process delays the arrival of tsunamis and greatly mitigates their impact on coastal communities.

4 Model Testing

We validate the forecast model for accuracy and robustness before it is integrated into the tsunami forecast system. Model accuracy determines the reliability of forecast. A numerical model may become unstable in cases of very high or very low wave heights, and must be avoided before the model is deployed in operation.

4.1 Accuracy

Factors that affect the accuracy of a forecast model include the topography and bathymetry, as well as grid resolutions. It is straightforward that errors in topography and bathymetry can cause errors in computed wave heights inundation. The numerical scheme employed in MOST is accurate to the second-order in space and first-order in time. Larger grid spacing can introduce higher numerical errors. Theoretically, higher resolution is desired regarding accuracy. On the other hand, numerical models at higher resolutions consume more computational resources. In developing a tsunami forecast model, we choose a resolution that maintains due accuracy and meanwhile requires a CPU time not exceeding the specific limit, i.e., 10 minutes for a 4-hour simulation.

To validate a numerical model, we can simulate historical events with this model and compare its results with those measured in field. The Myrtle Beach area lacks records of past tsunami events. Instead, we employ a series of synthetic scenarios and compare the numerical results between the reference and forecast models. This helps check the effects of numerical errors. The synthetic scenarios we employ in this study include 6 mega tsunamis, a tsunami generated by an Mw 7.5 earthquake, and a micro tsunami (Table 2). The epicenters of triggering earthquakes of the mega tsunamis are presented in Figure 3.

In Figures 4–11, we present the numerical results of synthetic scenarios. Comparison between the two models shows a good consistence in the distributed maximum water surface elevations in all 3 grids, as well as the time-series of water levels at the tide gage. We note some minor differences in wave heights and inundated areas between the two models. They are mainly due to the different resolutions. For the purpose of operational forecast, we believe the accuracy of the forecast model is sufficient.

Although all mega tsunami scenarios are due to earthquakes of same magnitude, their impacts on Myrtle Beach are very different. The highest wave heights and most severe coastal inundation are observed in the scenario of ATSZ 48-57. In this scenario, water waves are generated along the northeast edge of the Caribbean Plate and propagate into the Myrtle Beach area without significant interference from islands in their passage. In the scenarios of ATSZ 68-77 and ATSZ 82-91, most water waves are blocked by the Greater Antilles and may not bring considerable damage to the U.S. coasts. In another mega tsunami scenario, SSSZ 1-10, the tsunami source is too far way to pose a threat for Myrtle Beach.

4.2 Stability

The 6 mega tsunami scenarios represent events of extremely low probability. In recent centuries, such an event has not been observed in the Atlantic basin. In this study, no stability problem is observed in the 12-hour simulations of these scenarios. A numerical

model may also become unstable when the input wave heights are too low. In this situation, the amplitude of numerical errors may become larger than those of the water waves and current speeds, and increase rapidly until the computer memories become overflowed. In this study, we also test the forecast model for a micro tsunami scenario (SSSZ B11). To initiate real-time simulation of this scenario, we temporarily lower the required minimum input water surface displacement along the A-grid boundaries from 0.001 m to 0.00001 m. Computation of this scenario does not show instability either.

4.3   Sensitivity of bottom friction

Considering the wide continental shelf offshore the Myrtle Beach area, bottom friction may play a significant role in determining tsunami impacts. In MOST, energy dissipation due to bottom friction is approximated through the Manning roughness coefficient (Manning's n) in the depth-averaged momentum equations. The typical value of Manning's n is 0.03 in coastal waters (Bryant, 2001). The friction effects may be even stronger on dry land because of vegetation. The tsunami forecast system aims to guide tsunami-threatened communities in evacuation and mitigation. In this consideration, we employ a very low value of Manning's n to avoid underestimating the possible tsunami impact. In the Myrtle Beach model, this value is set to 0.01.

In order to show the effects of bottom friction, all synthetic tsunami scenarios are also simulated with $n = 0.03$. These results are presented in Figure 12, compared with the original ones computed with $n = 0.01$. Big differences are observed in scenarios of ATSZ 38-47 and ATSZ 48-57, where wave heights are large. In the other scenarios, this difference is smaller as the wave heights are lower.

5   Conclusions

In this report, we develop a tsunami forecast model for Myrtle Beach, South Carolina. This model is to be integrated into NOAA's tsunami forecast system that provides real-time forecast of tsunami arrival time, wave heights and coastal inundation for at-risk communities in the U.S. The core of the forecast model is a numerical model, which conducts real-time simulations of tsunami propagation and inundation in 3 telescoped nested grids constructed with the best available bathymetry and topography. The population and economic center of Myrtle Beach is covered by the innermost C-grid at a resolution of $3''$ (~ 93 m). The present model is configured to run a 12-hr simulation in less than 7 minutes of CPU time on a 2×6 core @ 2.93 GHz computer in linux 64 RH4 environment.

There are no historical data of tsunami hazards in the Myrtle Beach area. The forecast model is validated in synthetic tsunami scenarios by comparing its results with those from a higher-resolution reference model. Good agreement is observed between the two models, indicating negligible numerical errors even with reduced resolution in the forecast model. This study also indicates that the forecast model has a good numerical stability in both mega and micro tsunami scenarios. We further note that a potential megathrust event along the northeast edge of the Caribbean Plate may bring severe tsunami impact to Myrtle Beach. In such an event, water waves of wave heights exceeding 5 m may reach the coast, and a large area of land will be flooded.

Acknowledgement

References

Bryant, E. (2001), Tsunami: the Underrated Hazard, Cambridge University Press, 320 pp.

Driscol, N. W., Weissel, J. K., and Goff, J. A. (2000), Potential for large-scale submarine slope failure and tsunami generation along the U.S. mid-Atlantic coast, *Geology*, *20*(5), 4407–4410.

Gica, E., Spillane, M. C., Titov, V. V., Chamberlin, C. D., and Newman, J. C. (2008), Development of the forecast propagation database for NOAAs Short-Term Inundation Forecast for Tsunamis (SIFT), *NOAA Tech. Memo. OAR PMEL-139*, Pacific Marine Environmental Laboratory, NOAA, Seattle, WA, 89 pp.

Løvholt, F., Pedersen, G., and Gisler, G. (2008), Oceanic propagation of a potential tsunami from the La Palma Island, *J. Geophys. Res.*, 113, C09026, doi:10.1029/2007JC004603.

Percival, D. B., Arcas, D., Denbo, D. W., Eble, M. C., Gica, E., Mofjeld, H. O., Spillane, M. C., Tang, L., and Titov, V. V. (2009), Extracting tsunami source parameters via inversion of DART buoy data, *NOAA Tech. Memo. OAR PMEL-144*, Pacific Marine Environmental Laboratory, NOAA, Seattle, WA, 22 pp.

Percival, D. B., Denbo, D. W., Eble, M. C., Gica, E., Mofjeld, H. O., Spillane, M. C., Tang, L., and Titov, V. V. (2011), Extraction of tsunami source coefficients via inversion of DART®buoy data, *Nat. Hazards*, *58*(1), doi: 10.1007/s11069-010-9688-1, 567–590.

Storrs, C. (2009), Slip-sliding away: Myrtle Beach erosion could explain sand loss along the U.S. east coast, *Scientific American*, http://www.scientificamerican.com/article.cfm?id= myrtle-beach-south-carolina-coastline-erosion.

Synolakis, C. E., Bernard, E. N., Titov, V. V., Kânoğlu, U., and González, F. I. (2008), Validation and verification of tsunami numerical models, *Pure Appli. Geophys.*, 165(11-12), 2197–2228.

Tang, L., Titov, V. V., Wei, Y., Mofjeld, H. O., Spillane, M., Arcas, D., Bernard, E. N., Chamberlin, C. D., Gica, E., and Newman, J. (2008), Tsunami forecast analysis for the May 2006 Tonga tsunami, *J. Geophys. Res.*, *113*, C12015, doi: 10.1029/2008JC004922.

Tang L., Titov, V. V., and Chamberlin, C. D. (2009), Development, testing, and applications of site-specific tsunami inundation models for real-time forecasting, *J. Geophys. Res.*, *6*, doi: 10.1029/2009JC005476.

Ten Brink, U., Twichell, D., Geist, E., Chaytor, J., Locat, J., Lee, H., Buczkowski, B., Barkan, R., Solow, A., Andrews, B., Parsons, T., Lynett, P., Lin, J., and Sansoucy, M. (2008), Evaluation of tsunami sources with the potential to impact the U.S. Atlantic and Gulf coasts, USGS Administrative Report to the Nuclear Regulatory Commission, 300 pp.

Titov, V. V. and González, F. I. (1997), Implementation and testing of the Method of Splitting Tsunami (MOST) model, *NOAA Tech. Memo, ERL PMEL-112*, Pacific Marine Environmental Laboratory, NOAA, Seattle, WA, 11 pp.

Titov V. V., González F. I., Bernard E. N., Eble M. C., Mofjeld H. O., Newman J. C., Venturato A. J. (2005), Real-time tsunami forecasting: challenges and solutions, *Nat. Hazards*, 35, 41–58.

Titov, V. V. (2009), Tsunami forecasting. In: E. N. Bernard and A. R. Robinson (edited) *The Sea*, Vol. 15, Chapter 12, Harvard University Press, Cambridge, MA, and London, U.K., 371–400.

U.S. Census Bureau (2013), *State and County Quickfacts: Myrtle Beach (city), South Carolina*, retrieved May 3, 2013, from http://quickfacts.census.gov.

Wei, Y., Bernard, E. N., Tang, L., Weiss, R., Titov, V. V., Moore, C., Spillane, M., Hopkins, M., and Kânoğlu, U. (2008), Real-time experimental forecast of the Peruvian tsunami of August 2007 for U.S. coastlines, *Geophys. Res. Lett.*, *35*, L04609, doi:10.1029/2007GL032250.

Zhou, H., Moore, C. W., Wei, Y., and Titov, V. V. (2011), A nested-grid Boussinesq-type approach to modelling dispersive propagation and runup of landslide-generated tsunamis, *Nat. Hazards Earth Syst. Sci.*, *11*(10), doi: 10.5194/nhess-11-2677-2011, 2677–2697.
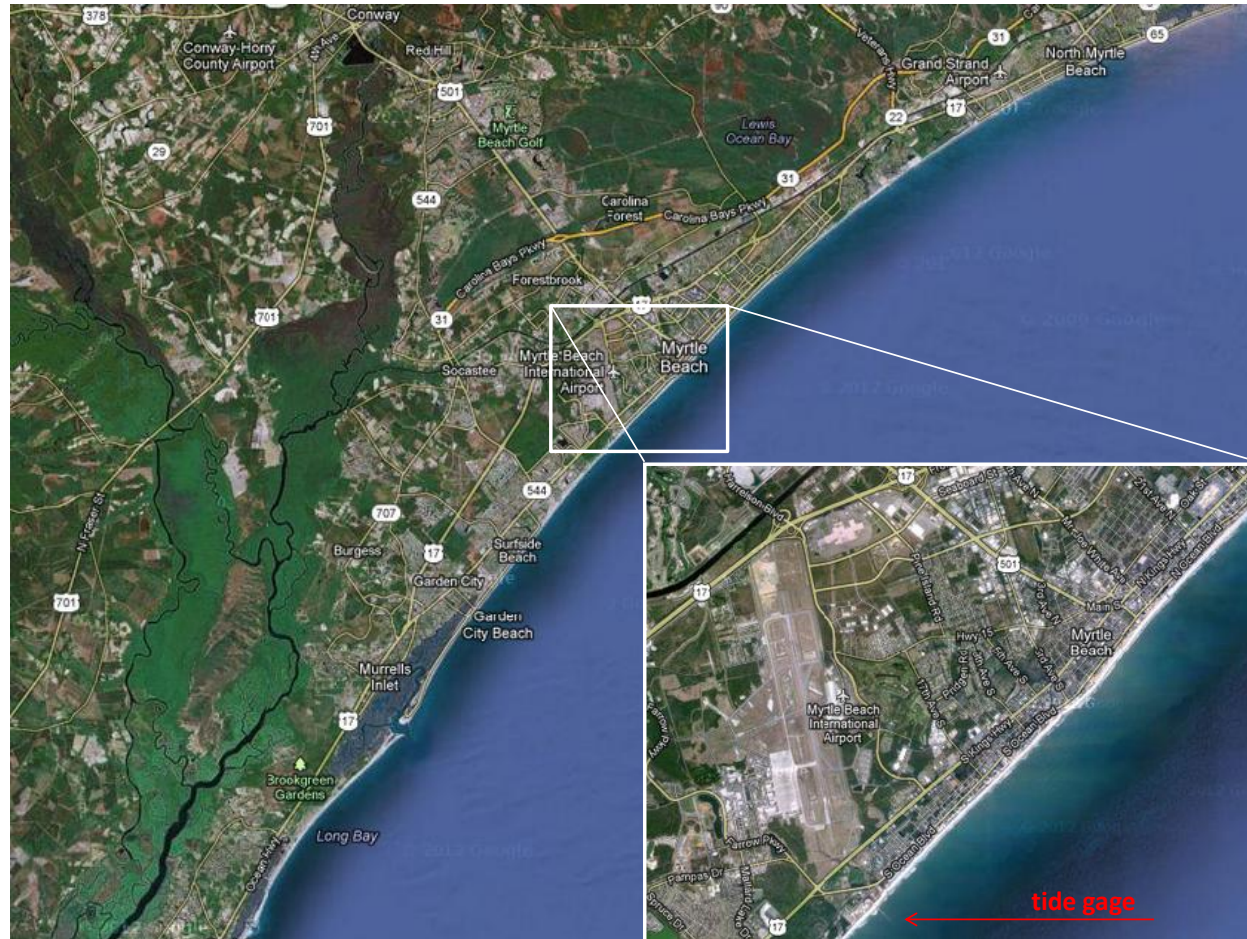
Figure 1: Location of Myrtle Beach, South Carolina (courtesy of "Google Maps").
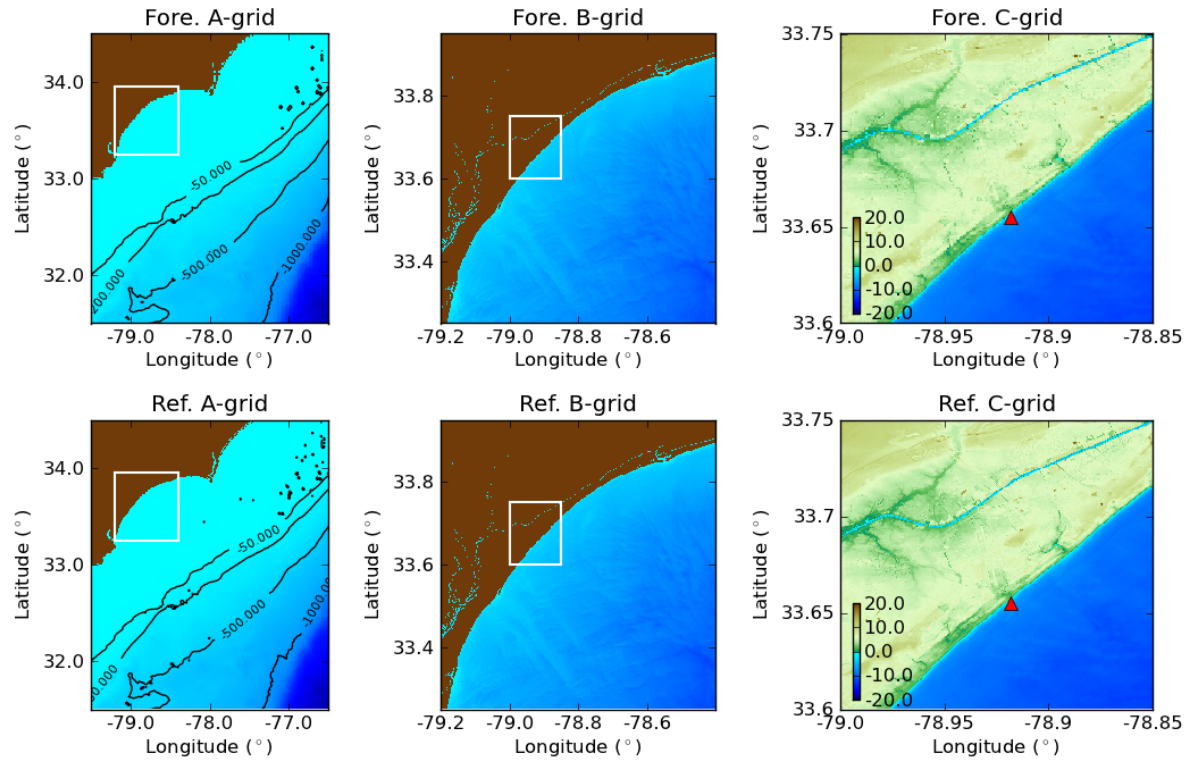
Figure 2: Domain coverage of computational grids in the forecast and reference models for Myrtle Beach, SC. Topography in A- and B-grids are not presented. Contours of -50, -200, -500, and -1000 m are plotted in A-grids with black lines. The tide gage is denoted as a triangle in C-grids.
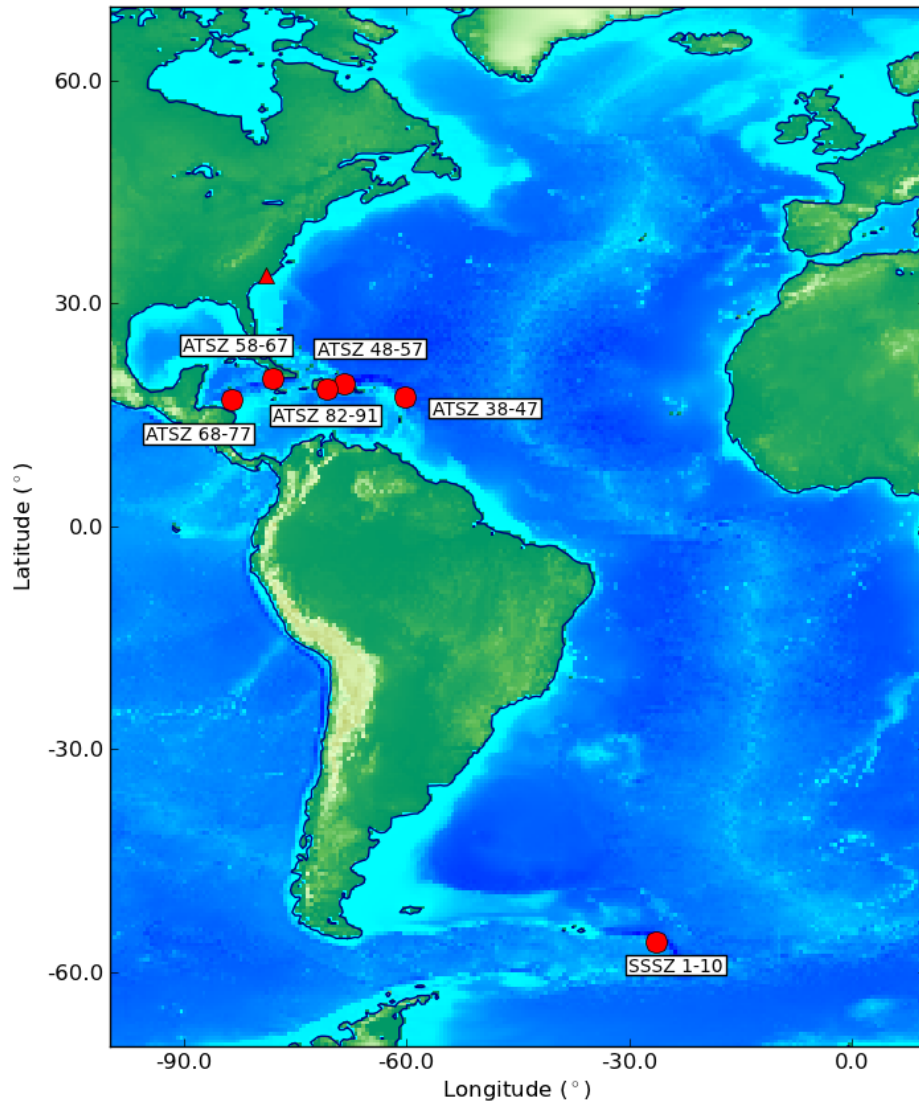
Figure 3: Epicenters of triggering earthquakes in synthetic mega tsunami scenarios employed to test the Myrtle Beach, SC forecast and reference models. Location of Myrtle Beach is indicated as a triangle in the map.

16
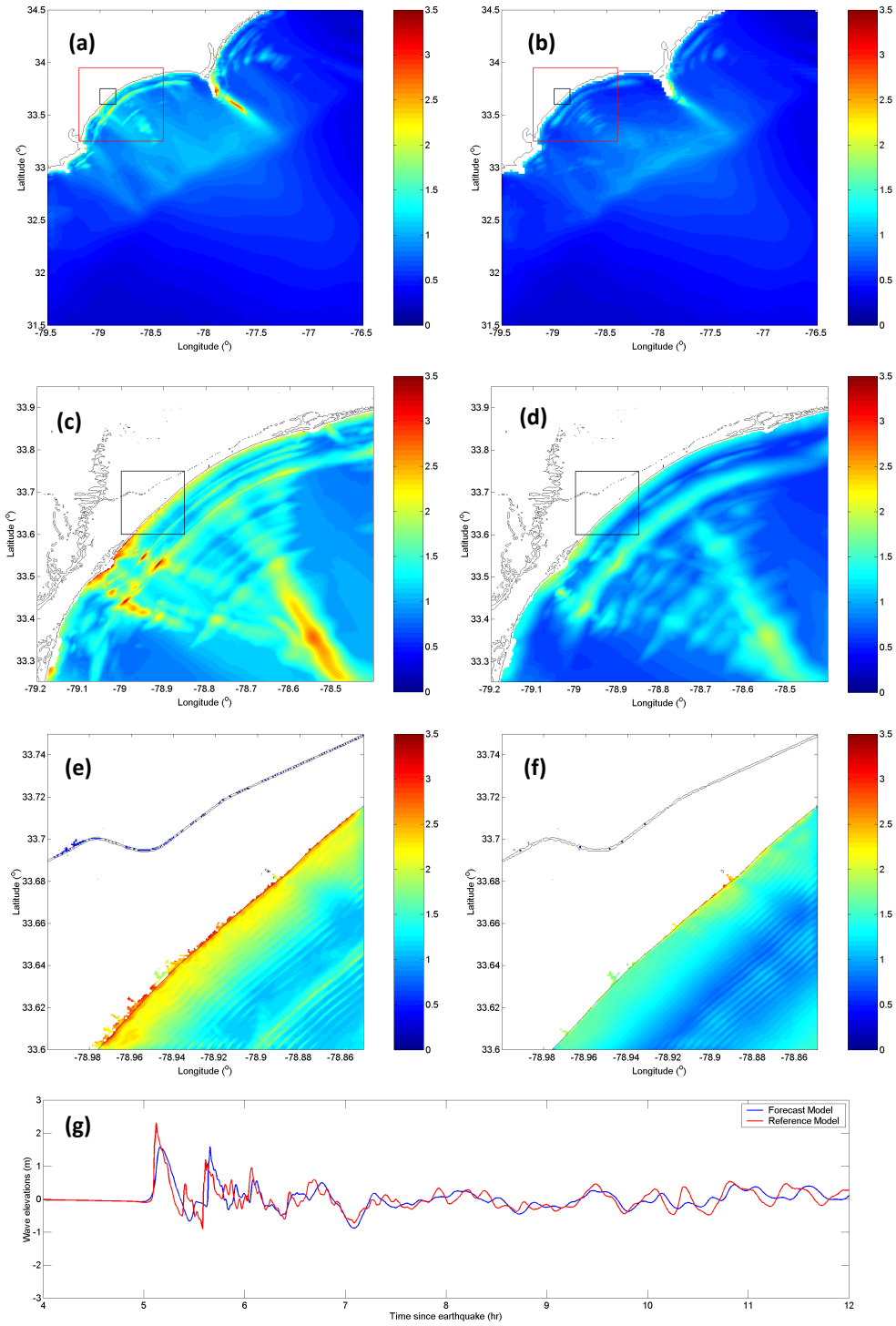
Figure 4: Model results for the synthetic scenario of ATSZ 38-47: maximum water surface elevations predicted by the reference model in A- (a), B- (c), and C-grids (e); maximum water surface elevations predicted by the forecast model in A- (b), B- (d), and C-grids (f); time-series of water surface elevations at the reference point (g). All water surface elevations are in meters.
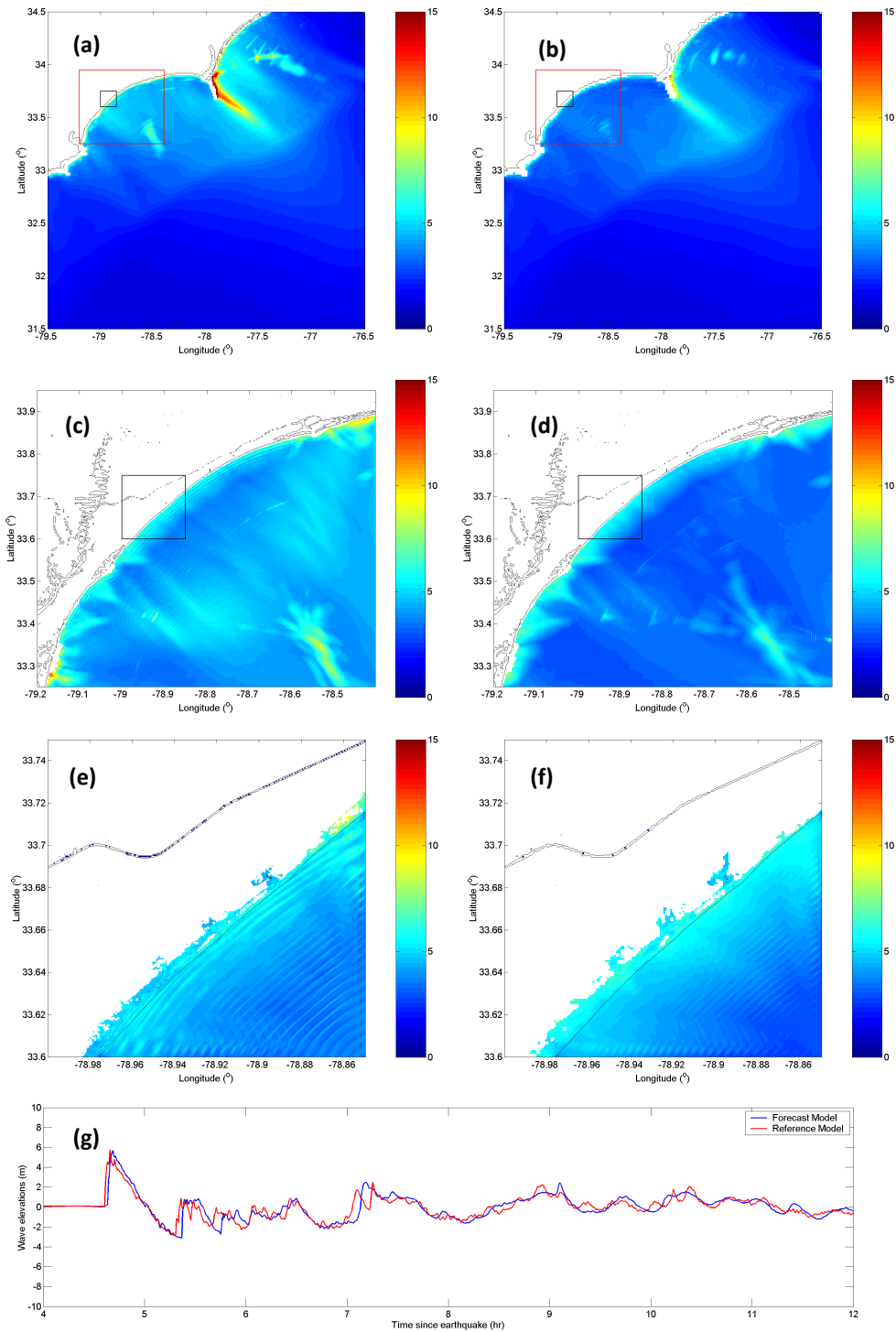
Figure 5: Model results for the synthetic scenario of ATSZ 48-57: maximum water surface elevations predicted by the reference model in A- (a), B- (c), and C-grids (e); maximum water surface elevations predicted by the forecast model in A- (b), B- (d), and C-grids (f); time-series of water surface elevations at the reference point (g). All water surface elevations are in meters.

18
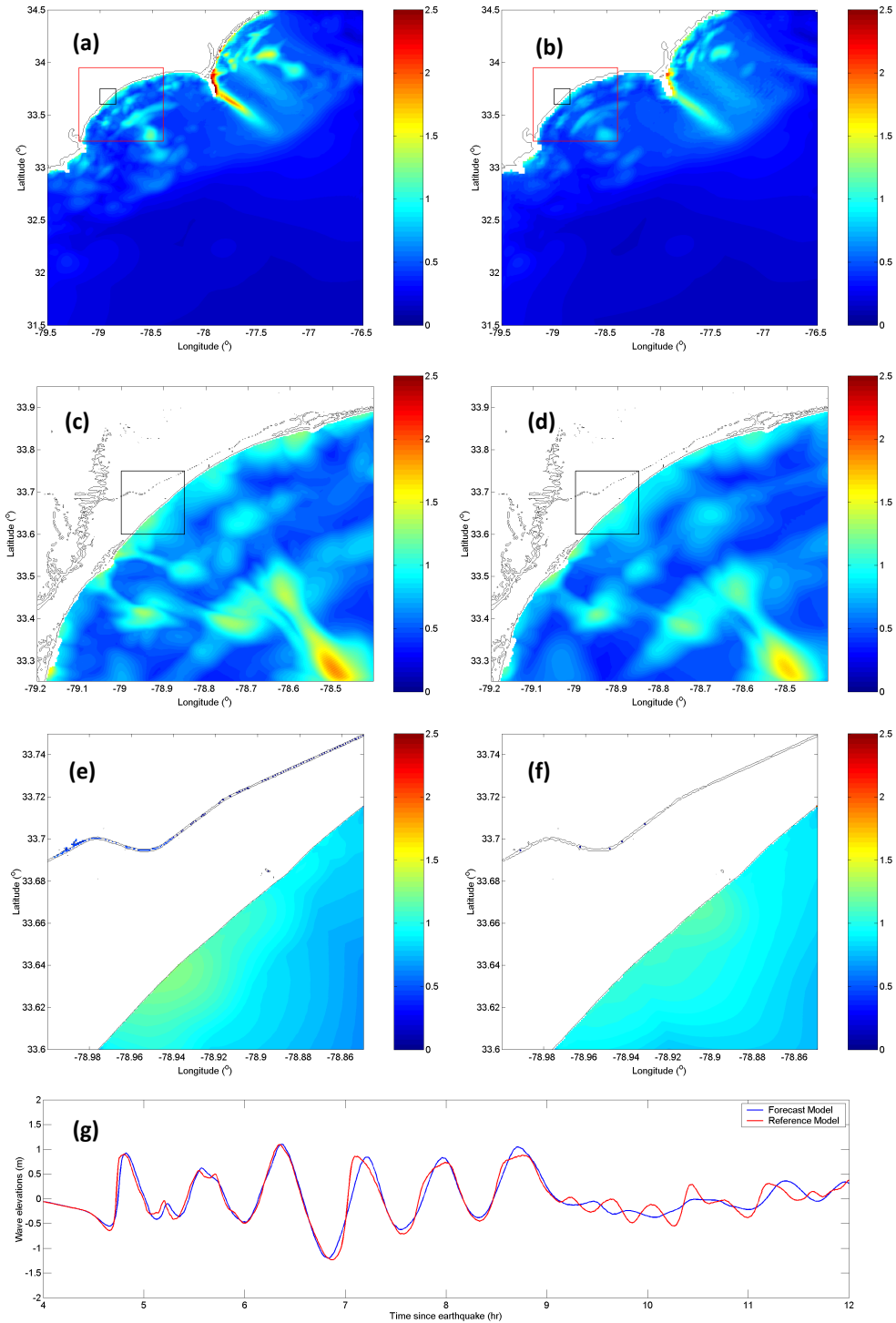
Figure 6: Model results for the synthetic scenario of ATSZ 58-67: maximum water surface elevations predicted by the reference model in A- (a), B- (c), and C-grids (e); maximum water surface elevations predicted by the forecast model in A- (b), B- (d), and C-grids (f); time-series of water surface elevations at the reference point (g). All water surface elevations are in meters.

19
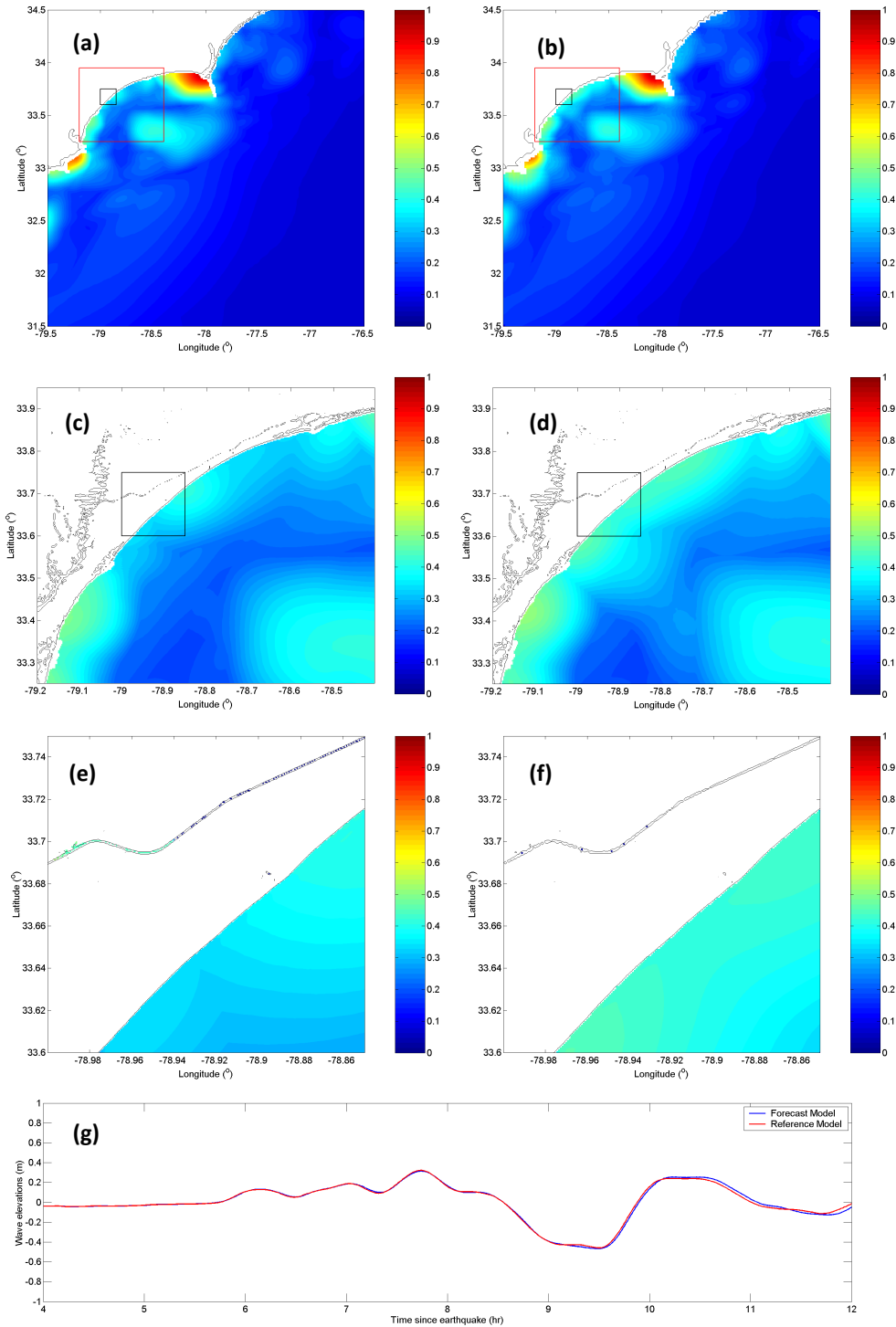
Figure 7: Model results for the synthetic scenario of ATSZ 68-77: maximum water surface elevations predicted by the reference model in A- (a), B- (c), and C-grids (e); maximum water surface elevations predicted by the forecast model in A- (b), B- (d), and C-grids (f); time-series of water surface elevations at the reference point (g). All water surface elevations are in meters.
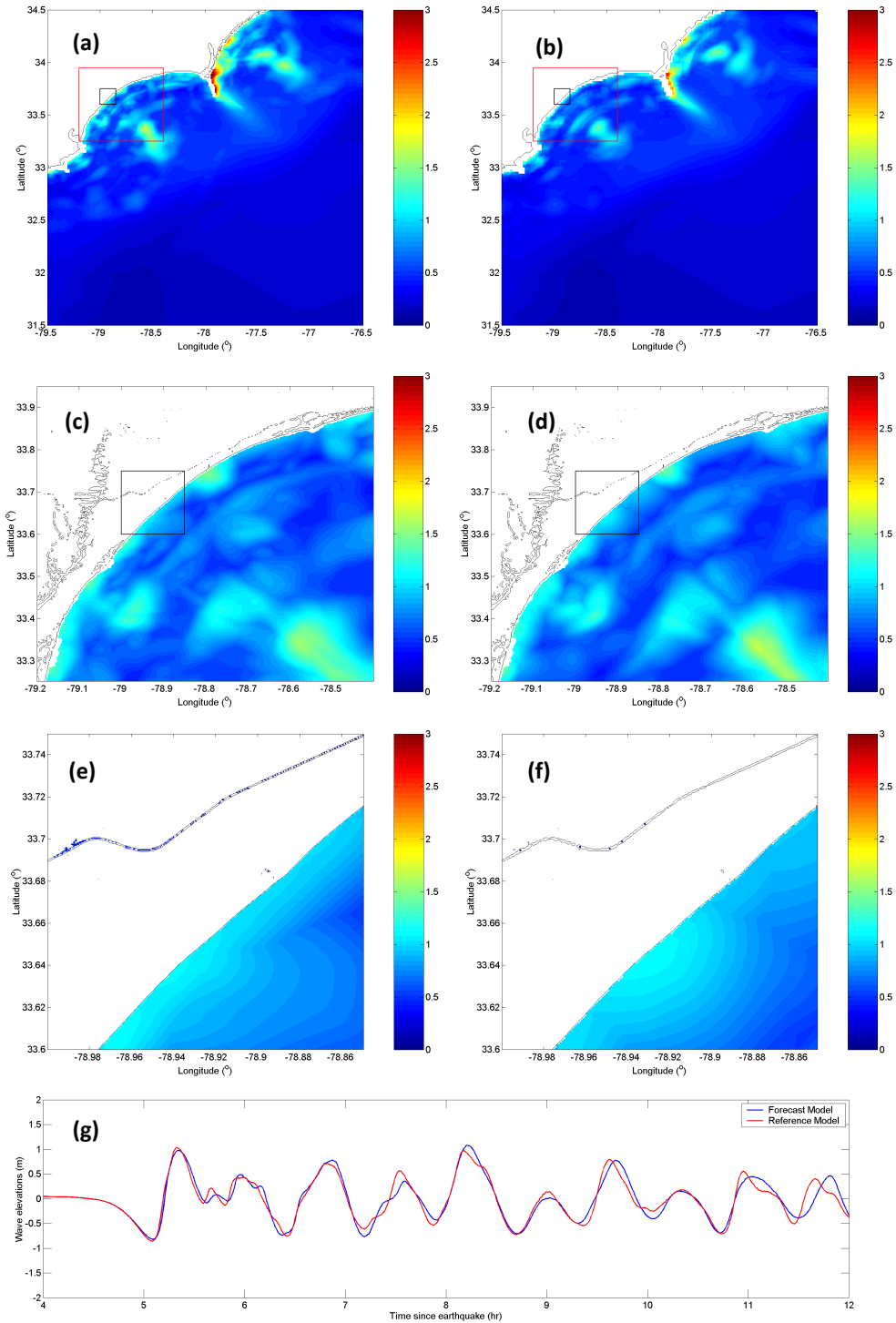
Figure 8: Model results for the synthetic scenario of ATSZ 82-91: maximum water surface elevations predicted by the reference model in A- (a), B- (c), and C-grids (e); maximum water surface elevations predicted by the forecast model in A- (b), B- (d), and C-grids (f); time-series of water surface elevations at the reference point (g). All water surface elevations are in meters.

21
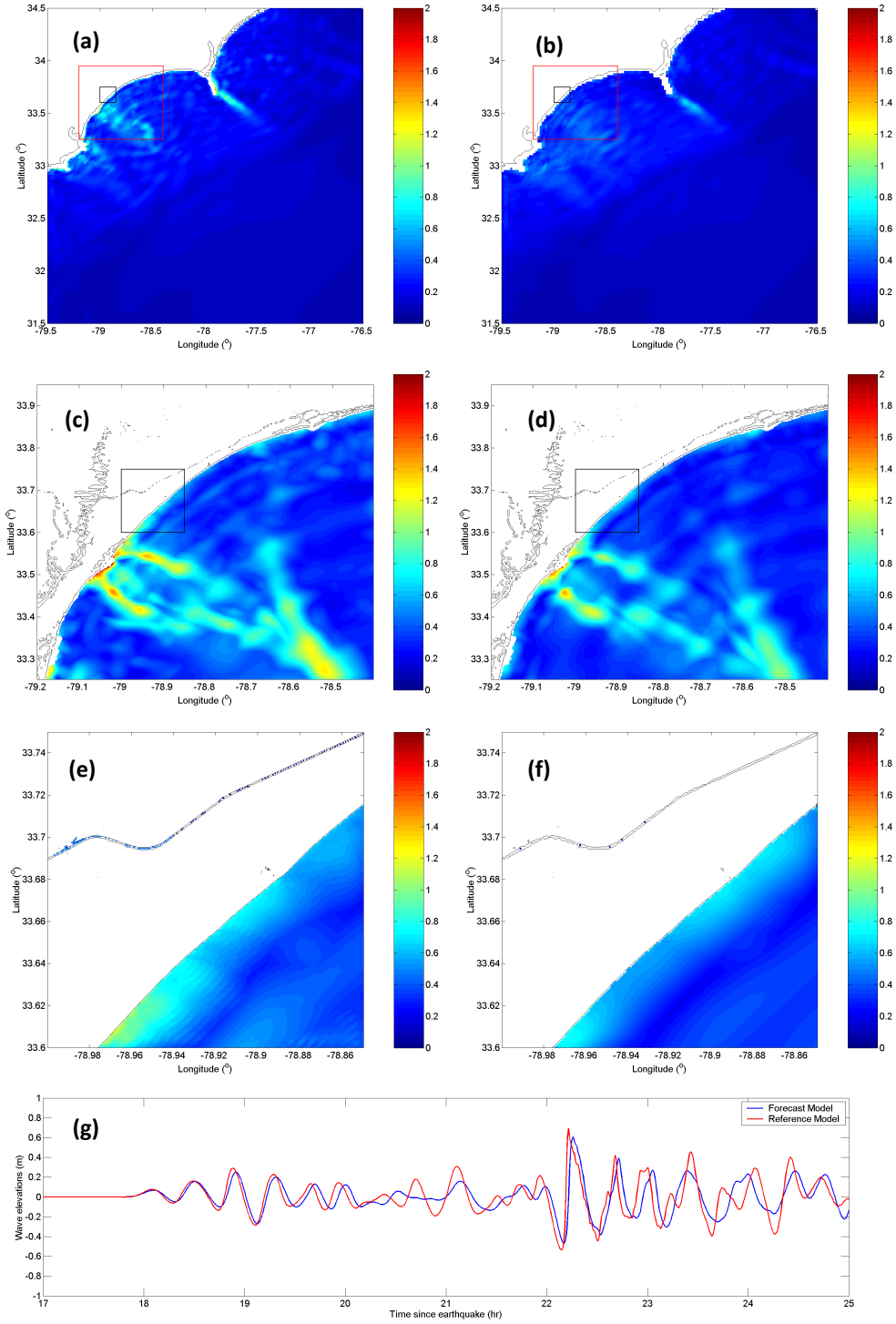
Figure 9: Model results for the synthetic scenario of SSSZ 1-10: maximum water surface elevations predicted by the reference model in A- (a), B- (c), and C-grids (e); maximum water surface elevations predicted by the forecast model in A- (b), B- (d), and C-grids (f); time-series of water surface elevations at the reference point (g). All water surface elevations are in meters.

22
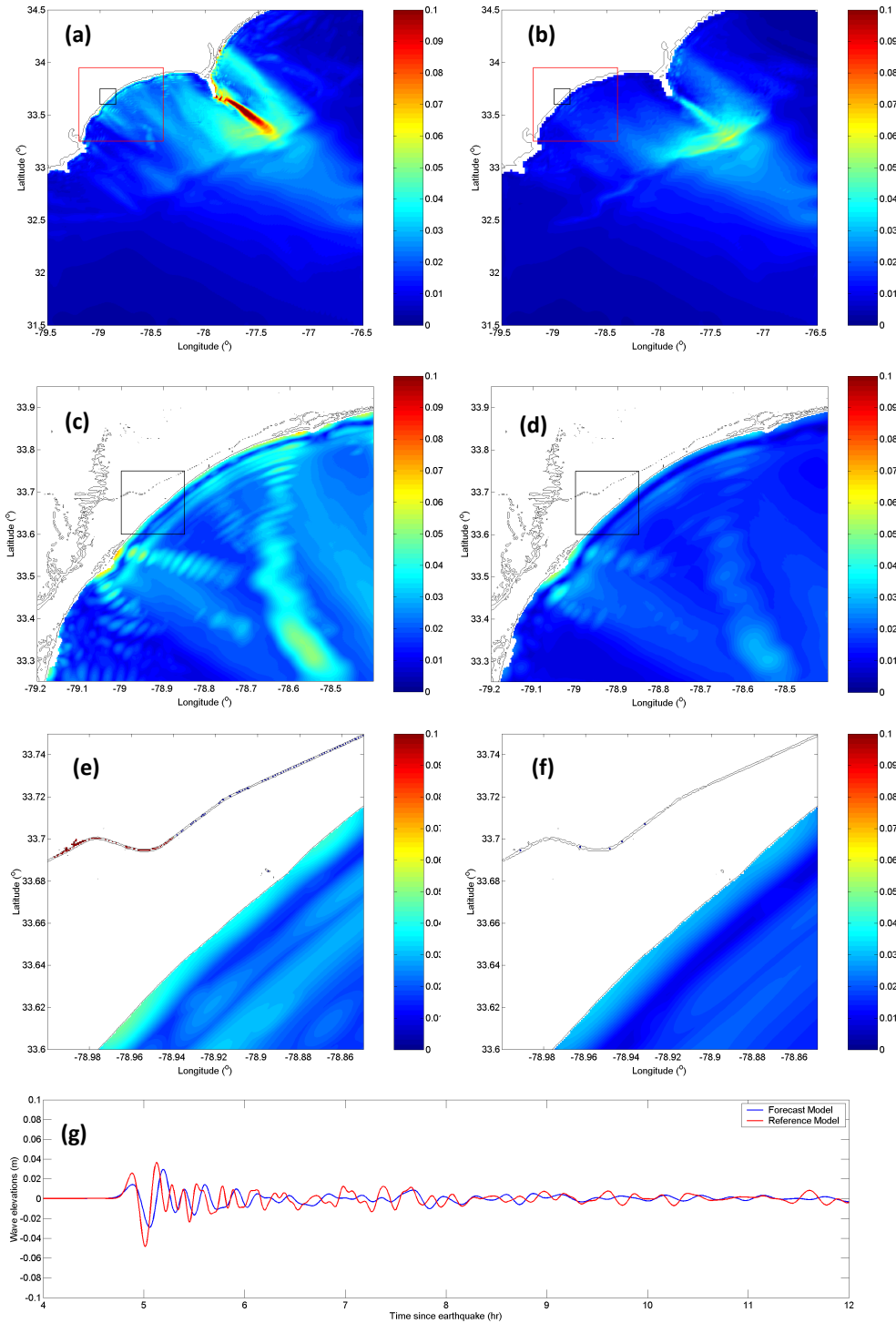
Figure 10: Model results for the synthetic scenario of ATSZ B52: maximum water surface elevations predicted by the reference model in A- (a), B- (c), and C-grids (e); maximum water surface elevations predicted by the forecast model in A- (b), B- (d), and C-grids (f); time-series of water surface elevations at the reference point (g). All water surface elevations are in meters.

23
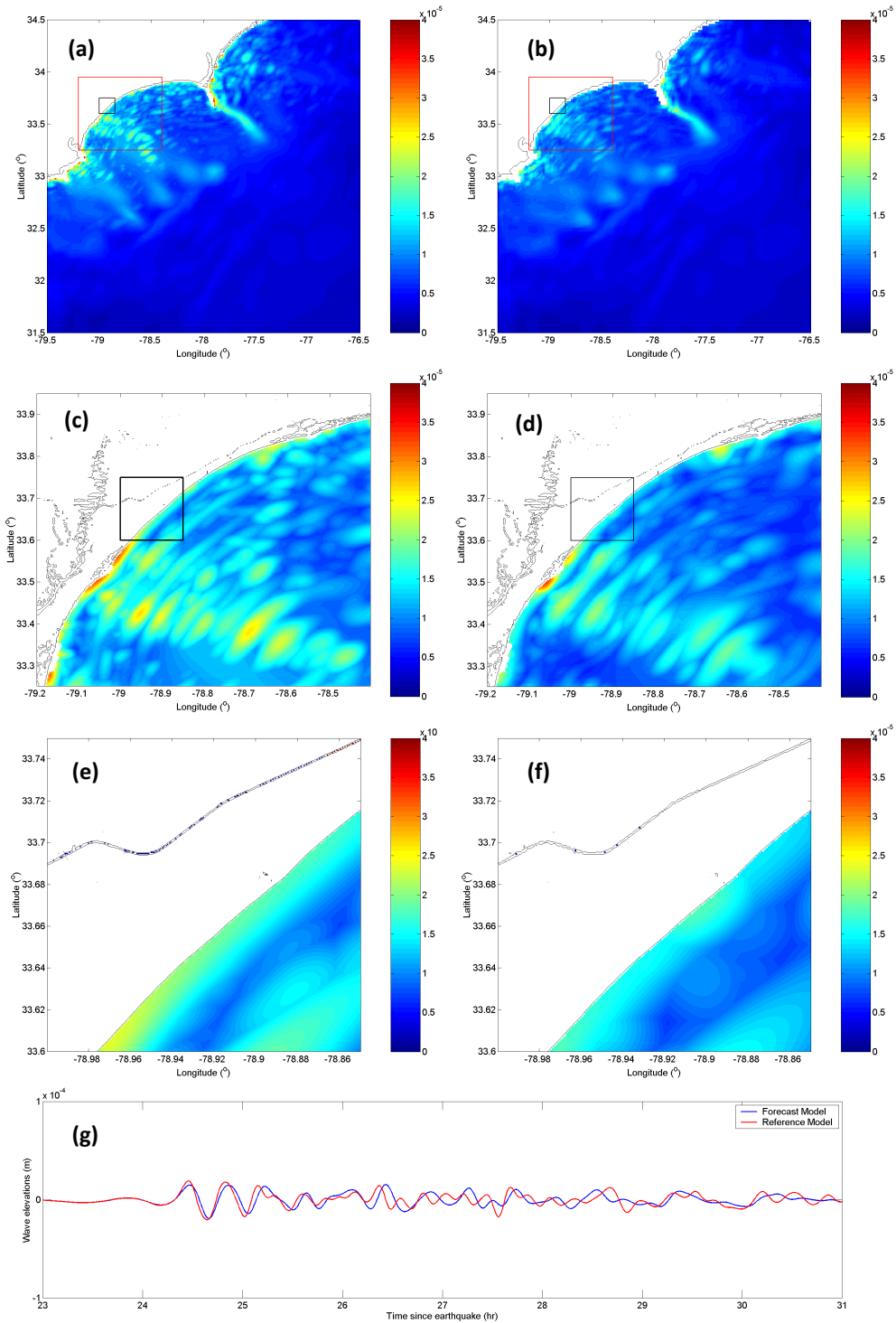
Figure 11: Model results for the synthetic scenario of SSSZ B11: maximum water surface elevations predicted by the reference model in A- (a), B- (c), and C-grids (e); maximum water surface elevations predicted by the forecast model in A- (b), B- (d), and C-grids (f); time-series of water surface elevations at the reference point (g). All water surface elevations are in meters.

24
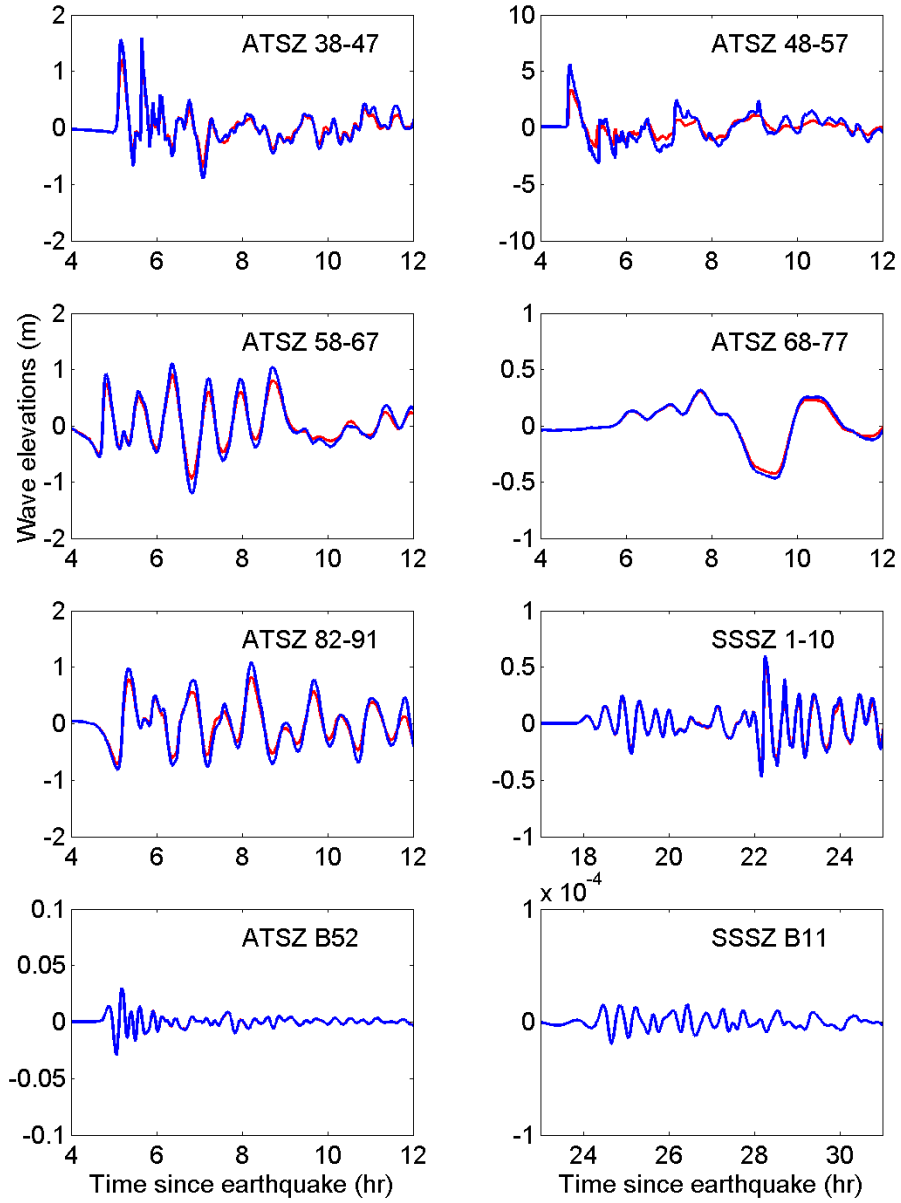
Figure 12: Effects of bottom friction on computed time-series of water surface elevations at the tide gage: n^2=0.0001 (blue) and 0.0009 (red).

Table 1: MOST setup of the reference and forecast models for Myrtle Beach, South Carolina.

Grid	Region	Reference Model Coverage Lat. (°N) Lon. (°W)	Cell Size	nx×ny	Time Step (sec.)	Forecast Model Coverage Lat. (°N) Lon. (°W)	Cell Size	nx×ny	Time Step (sec.)
A	South Carolina	31.5–34.5 79.5–76.5	36″	301×301	2.0	31.5–34.5 79.5–76.5	72″	151×151	8.8
B	Myrtle Beach	33.252–33.95 79.2–78.4025	9″	320×280	4.0	33.252–33.95 79.2–78.4025	9″	320×280	13.2
C	Myrtle Beach	33.60–33.75 79.0–78.85	2″	271×271	2.0	33.60–33.75 79.0–78.85	3″	181×181	4.4
Minimum offshore depth (m)					5.0				5.0
Water depth for dry land (m)					0.1				0.1
Friction coefficient (n^2)					0.0001				0.0001
CPU time for a 12-hr simulation					∼ 24 min				< 7 min

Note: All computations are conducted on a 2×6 core @2.93 GHz computer with 12 MB cache in linux 64 RH4 environment.

Table 2: Synthetic tsunami scenarios employed to test the Myrtle Beach, South Carolina reference and forecast models.

Scenorio No.	Scenario Name	Source Zone	Tsunami Source	α [m]
Mega-tsunami Scenario				
1	ATSZ 38-47	Atlantic	A38-A47, B38-B47	25
2	ATSZ 48-57	Atlantic	A48-A57, B48-B57	25
3	ATSZ 58-67	Atlantic	A58-A67, B58-B67	25
4	ATSZ 68-77	Atlantic	A68-A77, B68-B77	25
5	ATSZ 82-91	Atlantic	A82-A91, B82-B91	25
6	SSSZ 1-10	South Sandwich	A1-A10, B1-B10	25
Mw 7.5 Scenario				
7	ATSZ B52	Atlantic	B52	1
Micro-tsunami Scenario				
8	SSSZ B11	South Sandwich	B11	0.01

A Model *.in files for Myrtle Beach, South Carolina

A.1 Reference model *.in file

0.001	Minimum amp. of input offshore wave (m)
5.0	Minimum depth of offshore (m)
0.1	Dry land depth of inundation (m)
0.0001	Friction coefficient (n**2)
1	run up in a and b
300.0	max wave height meters
2.0	time step (sec)
21600	number of steps for 12 h simulation
1	Compute "A" arrays every n-th time step, n=
2	Compute "B" arrays every n-th time step, n=
16	Input number of steps between snapshots
0	...starting from
1	...saving grid every n-th node, n=

A.2 Forecast model *.in file

0.001	Minimum amp. of input offshore wave (m)
5.0	Minimum depth of offshore (m)
0.1	Dry land depth of inundation (m)
0.0001	Friction coefficient (n**2)
1	run up in a and b
300.0	max wave height meters
4.4	time step (sec)
11455	number of steps for 12 h simulation
2	Compute "A" arrays every n-th time step, n=
3	Compute "B" arrays every n-th time step, n=
6	Input number of steps between snapshots
0	...starting from
1	...saving grid every n-th node, n=

B   Propagation Database:
Atlantic Ocean Unit Sources
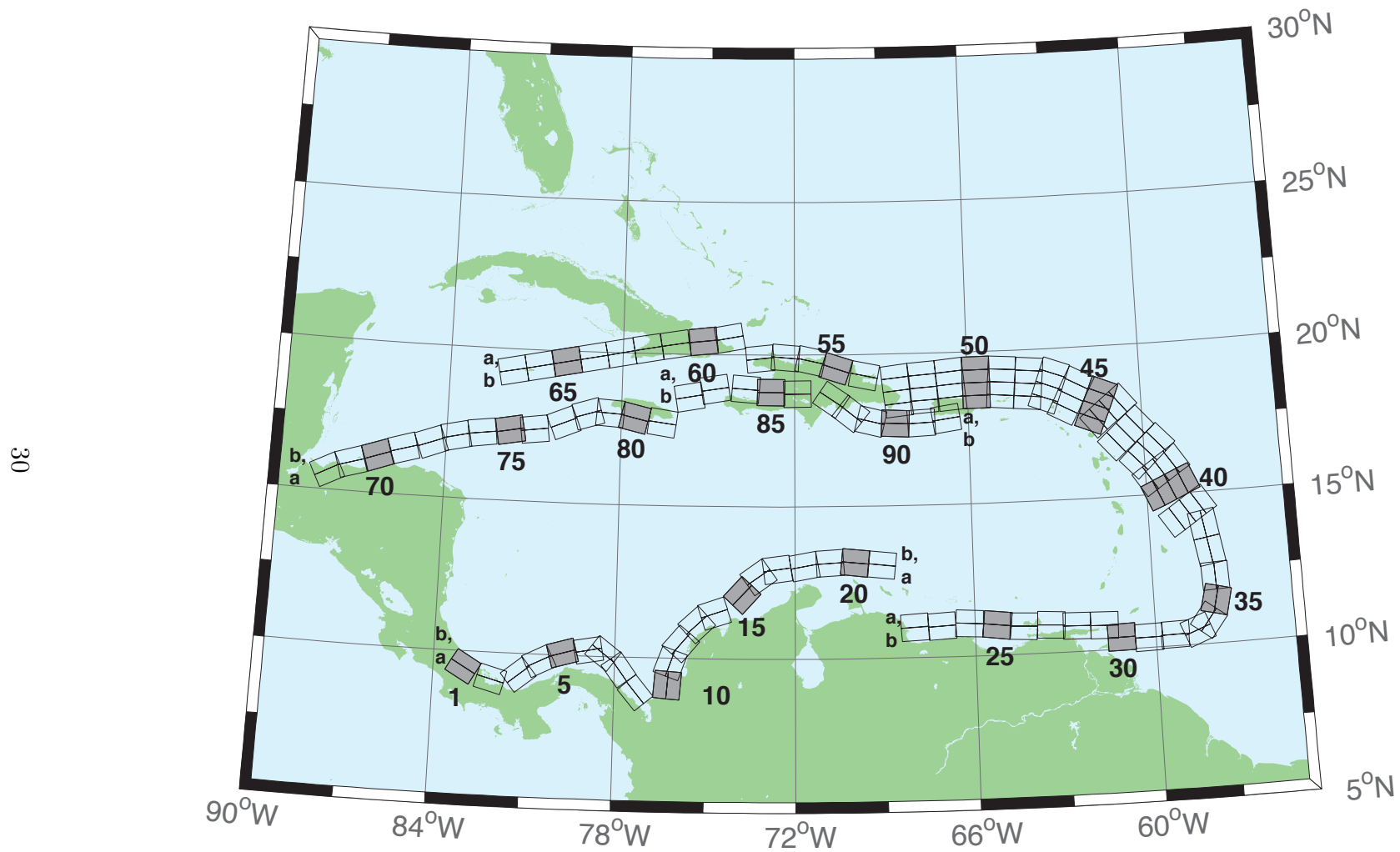
Figure B1: Atlantic Source Zone unit sources.

Table B1: Earthquake parameters for Atlantic Source Zone unit sources.

Segment	Description	Longitude(°E)	Latitude(°N)	Strike(°)	Dip(°)	Depth (km)
atsz–1a	Atlantic Source Zone	-83.2020	9.1449	120	27.5	28.09
atsz–1b	Atlantic Source Zone	-83.0000	9.4899	120	27.5	5
atsz–2a	Atlantic Source Zone	-82.1932	8.7408	105.1	27.5	28.09
atsz–2b	Atlantic Source Zone	-82.0880	9.1254	105.1	27.5	5
atsz–3a	Atlantic Source Zone	-80.9172	9.0103	51.31	30	30
atsz–3b	Atlantic Source Zone	-81.1636	9.3139	51.31	30	5
atsz–4a	Atlantic Source Zone	-80.3265	9.4308	63.49	30	30
atsz–4b	Atlantic Source Zone	-80.5027	9.7789	63.49	30	5
atsz–5a	Atlantic Source Zone	-79.6247	9.6961	74.44	30	30
atsz–5b	Atlantic Source Zone	-79.7307	10.0708	74.44	30	5
atsz–6a	Atlantic Source Zone	-78.8069	9.8083	79.71	30	30
atsz–6b	Atlantic Source Zone	-78.8775	10.1910	79.71	30	5
atsz–7a	Atlantic Source Zone	-78.6237	9.7963	127.2	30	30
atsz–7b	Atlantic Source Zone	-78.3845	10.1059	127.2	30	5
atsz–8a	Atlantic Source Zone	-78.1693	9.3544	143.8	30	30
atsz–8b	Atlantic Source Zone	-77.8511	9.5844	143.8	30	5
atsz–9a	Atlantic Source Zone	-77.5913	8.5989	139.9	30	30
atsz–9b	Atlantic Source Zone	-77.2900	8.8493	139.9	30	5
atsz–10a	Atlantic Source Zone	-75.8109	9.0881	4.67	17	19.62
atsz–10b	Atlantic Source Zone	-76.2445	9.1231	4.67	17	5
atsz–11a	Atlantic Source Zone	-75.7406	9.6929	19.67	17	19.62
atsz–11b	Atlantic Source Zone	-76.1511	9.8375	19.67	17	5
atsz–12a	Atlantic Source Zone	-75.4763	10.2042	40.4	17	19.62
atsz–12b	Atlantic Source Zone	-75.8089	10.4826	40.4	17	5
atsz–13a	Atlantic Source Zone	-74.9914	10.7914	47.17	17	19.62
atsz–13b	Atlantic Source Zone	-75.2890	11.1064	47.17	17	5
atsz–14a	Atlantic Source Zone	-74.5666	11.0708	71.68	17	19.62
atsz–14b	Atlantic Source Zone	-74.7043	11.4786	71.68	17	5
atsz–15a	Atlantic Source Zone	-73.4576	11.8012	42.69	17	19.62
atsz–15b	Atlantic Source Zone	-73.7805	12.0924	42.69	17	5
atsz–16a	Atlantic Source Zone	-72.9788	12.3365	54.75	17	19.62
atsz–16b	Atlantic Source Zone	-73.2329	12.6873	54.75	17	5
atsz–17a	Atlantic Source Zone	-72.5454	12.5061	81.96	17	19.62
atsz–17b	Atlantic Source Zone	-72.6071	12.9314	81.96	17	5
atsz–18a	Atlantic Source Zone	-71.6045	12.6174	79.63	17	19.62
atsz–18b	Atlantic Source Zone	-71.6839	13.0399	79.63	17	5
atsz–19a	Atlantic Source Zone	-70.7970	12.7078	86.32	17	19.62
atsz–19b	Atlantic Source Zone	-70.8253	13.1364	86.32	17	5
atsz–20a	Atlantic Source Zone	-70.0246	12.7185	95.94	17	19.62
atsz–20b	Atlantic Source Zone	-69.9789	13.1457	95.94	17	5
atsz–21a	Atlantic Source Zone	-69.1244	12.6320	95.94	17	19.62
atsz–21b	Atlantic Source Zone	-69.0788	13.0592	95.94	17	5
atsz–22a	Atlantic Source Zone	-68.0338	11.4286	266.9	15	17.94
atsz–22b	Atlantic Source Zone	-68.0102	10.9954	266.9	15	5
atsz–23a	Atlantic Source Zone	-67.1246	11.4487	266.9	15	17.94
atsz–23b	Atlantic Source Zone	-67.1010	11.0155	266.9	15	5
atsz–24a	Atlantic Source Zone	-66.1656	11.5055	273.3	15	17.94
atsz–24b	Atlantic Source Zone	-66.1911	11.0724	273.3	15	5
atsz–25a	Atlantic Source Zone	-65.2126	11.4246	276.4	15	17.94
atsz–25b	Atlantic Source Zone	-65.2616	10.9934	276.4	15	5
atsz–26a	Atlantic Source Zone	-64.3641	11.3516	272.9	15	17.94
atsz–26b	Atlantic Source Zone	-64.3862	10.9183	272.9	15	5
atsz–27a	Atlantic Source Zone	-63.4472	11.3516	272.9	15	17.94
atsz–27b	Atlantic Source Zone	-63.4698	10.9183	272.9	15	5
atsz–28a	Atlantic Source Zone	-62.6104	11.2831	271.1	15	17.94
atsz–28b	Atlantic Source Zone	-62.6189	10.8493	271.1	15	5
atsz–29a	Atlantic Source Zone	-61.6826	11.2518	271.6	15	17.94
atsz–29b	Atlantic Source Zone	-61.6947	10.8181	271.6	15	5
atsz–30a	Atlantic Source Zone	-61.1569	10.8303	269	15	17.94
atsz–30b	Atlantic Source Zone	-61.1493	10.3965	269	15	5
atsz–31a	Atlantic Source Zone	-60.2529	10.7739	269	15	17.94
atsz–31b	Atlantic Source Zone	-60.2453	10.3401	269	15	5
atsz–32a	Atlantic Source Zone	-59.3510	10.8123	269	15	17.94

Segment	Description	Longitude(°E)	Latitude(°N)	Strike(°)	Dip(°)	Depth (km)
atsz–32b	Atlantic Source Zone	-59.3734	10.3785	269	15	5
atsz–33a	Atlantic Source Zone	-58.7592	10.8785	248.6	15	17.94
atsz–33b	Atlantic Source Zone	-58.5984	10.4745	248.6	15	5
atsz–34a	Atlantic Source Zone	-58.5699	11.0330	217.2	15	17.94
atsz–34b	Atlantic Source Zone	-58.2179	10.7710	217.2	15	5
atsz–35a	Atlantic Source Zone	-58.3549	11.5300	193.7	15	17.94
atsz–35b	Atlantic Source Zone	-57.9248	11.4274	193.7	15	5
atsz–36a	Atlantic Source Zone	-58.3432	12.1858	177.7	15	17.94
atsz–36b	Atlantic Source Zone	-57.8997	12.2036	177.7	15	5
atsz–37a	Atlantic Source Zone	-58.4490	12.9725	170.7	15	17.94
atsz–37b	Atlantic Source Zone	-58.0095	13.0424	170.7	15	5
atsz–38a	Atlantic Source Zone	-58.6079	13.8503	170.2	15	17.94
atsz–38b	Atlantic Source Zone	-58.1674	13.9240	170.2	15	5
atsz–39a	Atlantic Source Zone	-58.6667	14.3915	146.8	15	17.94
atsz–39b	Atlantic Source Zone	-58.2913	14.6287	146.8	15	5
atsz–39y	Atlantic Source Zone	-59.4168	13.9171	146.8	15	43.82
atsz–39z	Atlantic Source Zone	-59.0415	14.1543	146.8	15	30.88
atsz–40a	Atlantic Source Zone	-59.1899	15.2143	156.2	15	17.94
atsz–40b	Atlantic Source Zone	-58.7781	15.3892	156.2	15	5
atsz–40y	Atlantic Source Zone	-60.0131	14.8646	156.2	15	43.82
atsz–40z	Atlantic Source Zone	-59.6012	15.0395	156.2	15	30.88
atsz–41a	Atlantic Source Zone	-59.4723	15.7987	146.3	15	17.94
atsz–41b	Atlantic Source Zone	-59.0966	16.0392	146.3	15	5
atsz–41y	Atlantic Source Zone	-60.2229	15.3177	146.3	15	43.82
atsz–41z	Atlantic Source Zone	-59.8473	15.5582	146.3	15	30.88
atsz–42a	Atlantic Source Zone	-59.9029	16.4535	137	15	17.94
atsz–42b	Atlantic Source Zone	-59.5716	16.7494	137	15	5
atsz–42y	Atlantic Source Zone	-60.5645	15.8616	137	15	43.82
atsz–42z	Atlantic Source Zone	-60.2334	16.1575	137	15	30.88
atsz–43a	Atlantic Source Zone	-60.5996	17.0903	138.7	15	17.94
atsz–43b	Atlantic Source Zone	-60.2580	17.3766	138.7	15	5
atsz–43y	Atlantic Source Zone	-61.2818	16.5177	138.7	15	43.82
atsz–43z	Atlantic Source Zone	-60.9404	16.8040	138.7	15	30.88
atsz–44a	Atlantic Source Zone	-61.1559	17.8560	141.1	15	17.94
atsz–44b	Atlantic Source Zone	-60.8008	18.1286	141.1	15	5
atsz–44y	Atlantic Source Zone	-61.8651	17.3108	141.1	15	43.82
atsz–44z	Atlantic Source Zone	-61.5102	17.5834	141.1	15	30.88
atsz–45a	Atlantic Source Zone	-61.5491	18.0566	112.8	15	17.94
atsz–45b	Atlantic Source Zone	-61.3716	18.4564	112.8	15	5
atsz–45y	Atlantic Source Zone	-61.9037	17.2569	112.8	15	43.82
atsz–45z	Atlantic Source Zone	-61.7260	17.6567	112.8	15	30.88
atsz–46a	Atlantic Source Zone	-62.4217	18.4149	117.9	15	17.94
atsz–46b	Atlantic Source Zone	-62.2075	18.7985	117.9	15	5
atsz–46y	Atlantic Source Zone	-62.8493	17.6477	117.9	15	43.82
atsz–46z	Atlantic Source Zone	-62.6352	18.0313	117.9	15	30.88
atsz–47a	Atlantic Source Zone	-63.1649	18.7844	110.5	20	22.1
atsz–47b	Atlantic Source Zone	-63.0087	19.1798	110.5	20	5
atsz–47y	Atlantic Source Zone	-63.4770	17.9936	110.5	20	56.3
atsz–47z	Atlantic Source Zone	-63.3205	18.3890	110.5	20	39.2
atsz–48a	Atlantic Source Zone	-63.8800	18.8870	95.37	20	22.1
atsz–48b	Atlantic Source Zone	-63.8382	19.3072	95.37	20	5
atsz–48y	Atlantic Source Zone	-63.9643	18.0465	95.37	20	56.3
atsz–48z	Atlantic Source Zone	-63.9216	18.4667	95.37	20	39.2
atsz–49a	Atlantic Source Zone	-64.8153	18.9650	94.34	20	22.1
atsz–49b	Atlantic Source Zone	-64.7814	19.3859	94.34	20	5
atsz–49y	Atlantic Source Zone	-64.8840	18.1233	94.34	20	56.3
atsz–49z	Atlantic Source Zone	-64.8492	18.5442	94.34	20	39.2
atsz–50a	Atlantic Source Zone	-65.6921	18.9848	89.59	20	22.1
atsz–50b	Atlantic Source Zone	-65.6953	19.4069	89.59	20	5
atsz–50y	Atlantic Source Zone	-65.6874	18.1407	89.59	20	56.3
atsz–50z	Atlantic Source Zone	-65.6887	18.5628	89.59	20	39.2
atsz–51a	Atlantic Source Zone	-66.5742	18.9484	84.98	20	22.1
atsz–51b	Atlantic Source Zone	-66.6133	19.3688	84.98	20	5
atsz–51y	Atlantic Source Zone	-66.4977	18.1076	84.98	20	56.3

Segment	Description	Longitude(°E)	Latitude(°N)	Strike(°)	Dip(°)	Depth (km)
atsz–51z	Atlantic Source Zone	-66.5353	18.5280	84.98	20	39.2
atsz–52a	Atlantic Source Zone	-67.5412	18.8738	85.87	20	22.1
atsz–52b	Atlantic Source Zone	-67.5734	19.2948	85.87	20	5
atsz–52y	Atlantic Source Zone	-67.4781	18.0319	85.87	20	56.3
atsz–52z	Atlantic Source Zone	-67.5090	18.4529	85.87	20	39.2
atsz–53a	Atlantic Source Zone	-68.4547	18.7853	83.64	20	22.1
atsz–53b	Atlantic Source Zone	-68.5042	19.2048	83.64	20	5
atsz–53y	Atlantic Source Zone	-68.3575	17.9463	83.64	20	56.3
atsz–53z	Atlantic Source Zone	-68.4055	18.3658	83.64	20	39.2
atsz–54a	Atlantic Source Zone	-69.6740	18.8841	101.5	20	22.1
atsz–54b	Atlantic Source Zone	-69.5846	19.2976	101.5	20	5
atsz–55a	Atlantic Source Zone	-70.7045	19.1376	108.2	20	22.1
atsz–55b	Atlantic Source Zone	-70.5647	19.5386	108.2	20	5
atsz–56a	Atlantic Source Zone	-71.5368	19.3853	102.6	20	22.1
atsz–56b	Atlantic Source Zone	-71.4386	19.7971	102.6	20	5
atsz–57a	Atlantic Source Zone	-72.3535	19.4838	94.2	20	22.1
atsz–57b	Atlantic Source Zone	-72.3206	19.9047	94.2	20	5
atsz–58a	Atlantic Source Zone	-73.1580	19.4498	84.34	20	22.1
atsz–58b	Atlantic Source Zone	-73.2022	19.8698	84.34	20	5
atsz–59a	Atlantic Source Zone	-74.3567	20.9620	259.7	20	22.1
atsz–59b	Atlantic Source Zone	-74.2764	20.5467	259.7	20	5
atsz–60a	Atlantic Source Zone	-75.2386	20.8622	264.2	15	17.94
atsz–60b	Atlantic Source Zone	-75.1917	20.4306	264.2	15	5
atsz–61a	Atlantic Source Zone	-76.2383	20.7425	260.7	15	17.94
atsz–61b	Atlantic Source Zone	-76.1635	20.3144	260.7	15	5
atsz–62a	Atlantic Source Zone	-77.2021	20.5910	259.9	15	17.94
atsz–62b	Atlantic Source Zone	-77.1214	20.1638	259.9	15	5
atsz–63a	Atlantic Source Zone	-78.1540	20.4189	259	15	17.94
atsz–63b	Atlantic Source Zone	-78.0661	19.9930	259	15	5
atsz–64a	Atlantic Source Zone	-79.0959	20.2498	259.2	15	17.94
atsz–64b	Atlantic Source Zone	-79.0098	19.8236	259.2	15	5
atsz–65a	Atlantic Source Zone	-80.0393	20.0773	258.9	15	17.94
atsz–65b	Atlantic Source Zone	-79.9502	19.6516	258.9	15	5
atsz–66a	Atlantic Source Zone	-80.9675	19.8993	258.6	15	17.94
atsz–66b	Atlantic Source Zone	-80.8766	19.4740	258.6	15	5
atsz–67a	Atlantic Source Zone	-81.9065	19.7214	258.5	15	17.94
atsz–67b	Atlantic Source Zone	-81.8149	19.2962	258.5	15	5
atsz–68a	Atlantic Source Zone	-87.8003	15.2509	62.69	15	17.94
atsz–68b	Atlantic Source Zone	-88.0070	15.6364	62.69	15	5
atsz–69a	Atlantic Source Zone	-87.0824	15.5331	72.73	15	17.94
atsz–69b	Atlantic Source Zone	-87.2163	15.9474	72.73	15	5
atsz–70a	Atlantic Source Zone	-86.1622	15.8274	70.64	15	17.94
atsz–70b	Atlantic Source Zone	-86.3120	16.2367	70.64	15	5
atsz–71a	Atlantic Source Zone	-85.3117	16.1052	73.7	15	17.94
atsz–71b	Atlantic Source Zone	-85.4387	16.5216	73.7	15	5
atsz–72a	Atlantic Source Zone	-84.3470	16.3820	69.66	15	17.94
atsz–72b	Atlantic Source Zone	-84.5045	16.7888	69.66	15	5
atsz–73a	Atlantic Source Zone	-83.5657	16.6196	77.36	15	17.94
atsz–73b	Atlantic Source Zone	-83.6650	17.0429	77.36	15	5
atsz–74a	Atlantic Source Zone	-82.7104	16.7695	82.35	15	17.94
atsz–74b	Atlantic Source Zone	-82.7709	17.1995	82.35	15	5
atsz–75a	Atlantic Source Zone	-81.7297	16.9003	79.86	15	17.94
atsz–75b	Atlantic Source Zone	-81.8097	17.3274	79.86	15	5
atsz–76a	Atlantic Source Zone	-80.9196	16.9495	82.95	15	17.94
atsz–76b	Atlantic Source Zone	-80.9754	17.3801	82.95	15	5
atsz–77a	Atlantic Source Zone	-79.8086	17.2357	67.95	15	17.94
atsz–77b	Atlantic Source Zone	-79.9795	17.6378	67.95	15	5
atsz–78a	Atlantic Source Zone	-79.0245	17.5415	73.61	15	17.94
atsz–78b	Atlantic Source Zone	-79.1532	17.9577	73.61	15	5
atsz–79a	Atlantic Source Zone	-78.4122	17.5689	94.07	15	17.94
atsz–79b	Atlantic Source Zone	-78.3798	18.0017	94.07	15	5
atsz–80a	Atlantic Source Zone	-77.6403	17.4391	103.3	15	17.94
atsz–80b	Atlantic Source Zone	-77.5352	17.8613	103.3	15	5
atsz–81a	Atlantic Source Zone	-76.6376	17.2984	98.21	15	17.94

Segment	Description	Longitude(°E)	Latitude(°N)	Strike(°)	Dip(°)	Depth (km)
atsz–81b	Atlantic Source Zone	-76.5726	17.7278	98.21	15	5
atsz–82a	Atlantic Source Zone	-75.7299	19.0217	260.1	15	17.94
atsz–82b	Atlantic Source Zone	-75.6516	18.5942	260.1	15	5
atsz–83a	Atlantic Source Zone	-74.8351	19.2911	260.8	15	17.94
atsz–83b	Atlantic Source Zone	-74.7621	18.8628	260.8	15	5
atsz–84a	Atlantic Source Zone	-73.6639	19.2991	274.8	15	17.94
atsz–84b	Atlantic Source Zone	-73.7026	18.8668	274.8	15	5
atsz–85a	Atlantic Source Zone	-72.8198	19.2019	270.6	15	17.94
atsz–85b	Atlantic Source Zone	-72.8246	18.7681	270.6	15	5
atsz–86a	Atlantic Source Zone	-71.9143	19.1477	269.1	15	17.94
atsz–86b	Atlantic Source Zone	-71.9068	18.7139	269.1	15	5
atsz–87a	Atlantic Source Zone	-70.4738	18.8821	304.5	15	17.94
atsz–87b	Atlantic Source Zone	-70.7329	18.5245	304.5	15	5
atsz–88a	Atlantic Source Zone	-69.7710	18.3902	308.9	15	17.94
atsz–88b	Atlantic Source Zone	-70.0547	18.0504	308.4	15	5
atsz–89a	Atlantic Source Zone	-69.2635	18.2099	283.9	15	17.94
atsz–89b	Atlantic Source Zone	-69.3728	17.7887	283.9	15	5
atsz–90a	Atlantic Source Zone	-68.5059	18.1443	272.9	15	17.94
atsz–90b	Atlantic Source Zone	-68.5284	17.7110	272.9	15	5
atsz–91a	Atlantic Source Zone	-67.6428	18.1438	267.8	15	17.94
atsz–91b	Atlantic Source Zone	-67.6256	17.7103	267.8	15	5
atsz–92a	Atlantic Source Zone	-66.8261	18.2536	262	15	17.94
atsz–92b	Atlantic Source Zone	-66.7627	17.8240	262	15	5
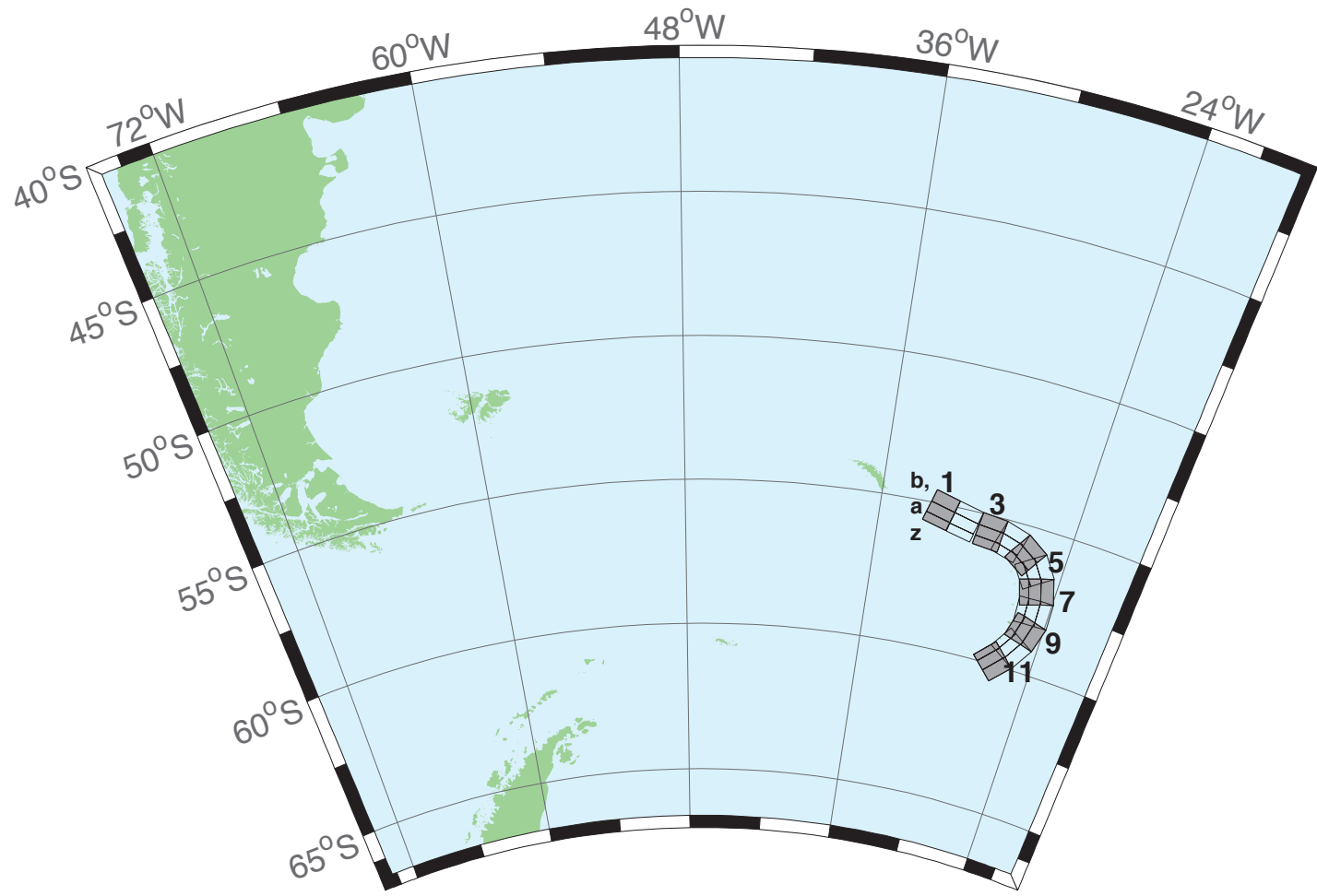
Figure B2: South Sandwich Islands Subduction Zone.

Table B2: Earthquake parameters for South Sandwich Islands Subduction Zone
unit sources.

Segment	Description	Longitude(°E)	Latitude(°N)	Strike(°)	Dip(°)	Depth (km)
sssz–1a	South Sandwich Islands Subduction Zone	-32.3713	-55.4655	104.7	28.53	17.51
sssz–1b	South Sandwich Islands Subduction Zone	-32.1953	-55.0832	104.7	9.957	8.866
sssz–1z	South Sandwich Islands Subduction Zone	-32.5091	-55.7624	104.7	46.99	41.39
sssz–2a	South Sandwich Islands Subduction Zone	-30.8028	-55.6842	102.4	28.53	17.51
sssz–2b	South Sandwich Islands Subduction Zone	-30.6524	-55.2982	102.4	9.957	8.866
sssz–2z	South Sandwich Islands Subduction Zone	-30.9206	-55.9839	102.4	46.99	41.39
sssz–3a	South Sandwich Islands Subduction Zone	-29.0824	-55.8403	95.53	28.53	17.51
sssz–3b	South Sandwich Islands Subduction Zone	-29.0149	-55.4468	95.53	9.957	8.866
sssz–3z	South Sandwich Islands Subduction Zone	-29.1353	-56.1458	95.53	46.99	41.39
sssz–4a	South Sandwich Islands Subduction Zone	-27.8128	-55.9796	106.1	28.53	17.51
sssz–4b	South Sandwich Islands Subduction Zone	-27.6174	-55.5999	106.1	9.957	8.866
sssz–4z	South Sandwich Islands Subduction Zone	-27.9659	-56.2744	106.1	46.99	41.39
sssz–5a	South Sandwich Islands Subduction Zone	-26.7928	-56.2481	123.1	28.53	17.51
sssz–5b	South Sandwich Islands Subduction Zone	-26.4059	-55.9170	123.1	9.957	8.866
sssz–5z	South Sandwich Islands Subduction Zone	-27.0955	-56.5052	123.1	46.99	41.39
sssz–6a	South Sandwich Islands Subduction Zone	-26.1317	-56.6466	145.6	23.28	16.11
sssz–6b	South Sandwich Islands Subduction Zone	-25.5131	-56.4133	145.6	9.09	8.228
sssz–6z	South Sandwich Islands Subduction Zone	-26.5920	-56.8194	145.6	47.15	35.87
sssz–7a	South Sandwich Islands Subduction Zone	-25.6787	-57.2162	162.9	21.21	14.23
sssz–7b	South Sandwich Islands Subduction Zone	-24.9394	-57.0932	162.9	7.596	7.626
sssz–7z	South Sandwich Islands Subduction Zone	-26.2493	-57.3109	162.9	44.16	32.32
sssz–8a	South Sandwich Islands Subduction Zone	-25.5161	-57.8712	178.2	20.33	15.91
sssz–8b	South Sandwich Islands Subduction Zone	-24.7233	-57.8580	178.2	8.449	8.562
sssz–8z	South Sandwich Islands Subduction Zone	-26.1280	-57.8813	178.2	43.65	33.28
sssz–9a	South Sandwich Islands Subduction Zone	-25.6657	-58.5053	195.4	25.76	15.71
sssz–9b	South Sandwich Islands Subduction Zone	-24.9168	-58.6127	195.4	8.254	8.537
sssz–9z	South Sandwich Islands Subduction Zone	-26.1799	-58.4313	195.4	51.69	37.44
sssz–10a	South Sandwich Islands Subduction Zone	-26.1563	-59.1048	212.5	32.82	15.65
sssz–10b	South Sandwich Islands Subduction Zone	-25.5335	-59.3080	212.5	10.45	6.581
sssz–10z	South Sandwich Islands Subduction Zone	-26.5817	-58.9653	212.5	54.77	42.75
sssz–11a	South Sandwich Islands Subduction Zone	-27.0794	-59.6799	224.2	33.67	15.75
sssz–11b	South Sandwich Islands Subduction Zone	-26.5460	-59.9412	224.2	11.32	5.927
sssz–11z	South Sandwich Islands Subduction Zone	-27.4245	-59.5098	224.2	57.19	43.46

C Forecast Model Testing

Author: Lindsey Wright

C.1 Purpose

Forecast models are tested with synthetic tsunami events covering a range of tsunami source locations and magnitudes. Testing is also done with selected historical tsunami events when available.

The purpose of forecast model testing is three-fold. The first objective is to assure that the results obtained with the NOAA's tsunami forecast system software, which has been released to the Tsunami Warning Centers for operational use, are consistent with those obtained by the researcher during the development of the forecast model. The second objective is to test the forecast model for consistency, accuracy, time efficiency, and quality of results over a range of possible tsunami locations and magnitudes. The third objective is to identify bugs and issues in need of resolution by the researcher who developed the Forecast Model or by the forecast system software development team before the next version release to NOAAs two Tsunami Warning Centers.

Local hardware and software applications, and tools familiar to the researcher(s), are used to run the Method of Splitting Tsunamis (MOST) model during the forecast model development. The test results presented in this report lend confidence that the model performs as developed and produces the same results when initiated within the forecast system application in an operational setting as those produced by the researcher during the forecast model development. The test results assure those who rely on the Myrtle Beach tsunami forecast model that consistent results are produced irrespective of system.

C.2 Testing Procedure

The general procedure for forecast model testing is to run a set of synthetic tsunami scenarios and a selected set of historical tsunami events through the forecast system application and compare the results with those obtained by the researcher during the forecast model development and presented in the Tsunami Forecast Model Report. Specific steps taken to test the model include:

1. Identification of testing scenarios, including the standard set of synthetic events, appropriate historical events, and customized synthetic scenarios that may have been used by the researcher(s) in developing the forecast model.

2. Creation of new events to represent customized synthetic scenarios used by the researcher(s) in developing the forecast model, if any.

3. Submission of test model runs with the forecast system, and export of the results from A, B, and C grids, along with time series.

4. Recording applicable metadata, including the specific forecast system version used for testing.

5. Examination of forecast model results for instabilities in both time series and plot results.

6. Comparison of forecast model results obtained through the forecast system with those obtained during the forecast model development.

7. Summarization of results with specific mention of quality, consistency, and time efficiency.

8. Reporting of issues identified to modeler and forecast system software development team.

9. Retesting the forecast models in the forecast system when reported issues have been addressed or explained.

Synthetic model runs were tested on a DELL PowerEdge R510 computer equipped with two Xeon E5670 processors at 2.93 Ghz, each with 12 MBytes of cache and 32GB memory. The processors are hex core and support hyperthreading, resulting in the computer performing as a 24 processor core machine. Additionally, the testing computer supports 10 Gigabit Ethernet for fast network connections. This computer configuration is similar or the same as the configurations of the computers installed at the Tsunami Warning Centers so the compute times should only vary slightly.

C.3   Results

The Myrtle Beach forecast model was tested with SIFT version 3.2.

The Myrtle Beach, South Carolina forecast model was tested with three synthetic scenarios. Test results from the forecast system and comparisons with the results obtained during the forecast model development are shown numerically in Table C1 and graphically in Figures C1 to C3. The results show that the minimum and maximum amplitudes and time series obtained from the forecast system agree with those obtained during the forecast model development, and that the forecast model is stable and robust, with consistent and high quality results across geographically distributed tsunami sources. The model run time (wall clock time) was less than 4.2 minutes for 13.9 hours of simulation time, and 1.2 minutes for 4.0 hours. This run time is within the 10 minute run time for 4 hours of simulation time and satisfies run time requirements.

A suite of three synthetic events was run on the Myrtle Beach forecast model. The modeled scenarios were stable for all cases run with no inconsistencies or ringing. The largest modeled height was 335 centimeters (cm) from the Atlantic (ATSZ 48-57) source zone. The smallest signal of 52 cm was recorded at the far field South Sandwich (SSSZ 1-10) source zone. Maximum and minimum values were not available from development but visual comparisons between the development cases and the forecast system output were consistent in shape and amplitude for all cases run. The Myrtle Beach reference point used for the forecast model development is the same as what is deployed in the forecast system, so the results can be considered valid for the three cases studied.
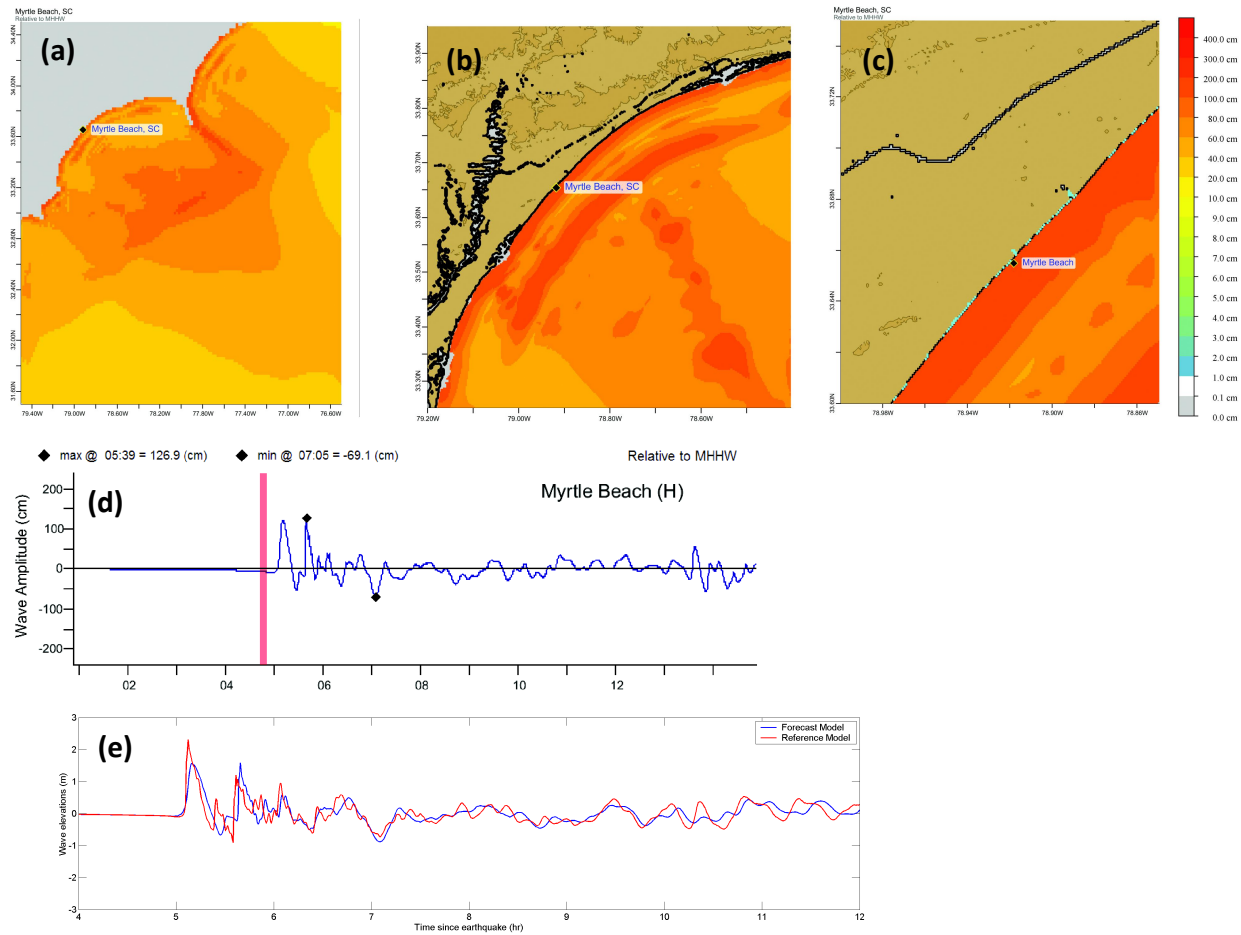
Figure C1: Response of the Myrtle Beach forecast model to synthetic scenario ATSZ 38-47 (α=25). Maximum sea surface elevation for (a) A-grid, b) B-grid, c) C-grid. Sea surface elevation time series at the C-grid warning point (d). The lower time series plot (e) is the result obtained during model development and is shown for comparison with test results.
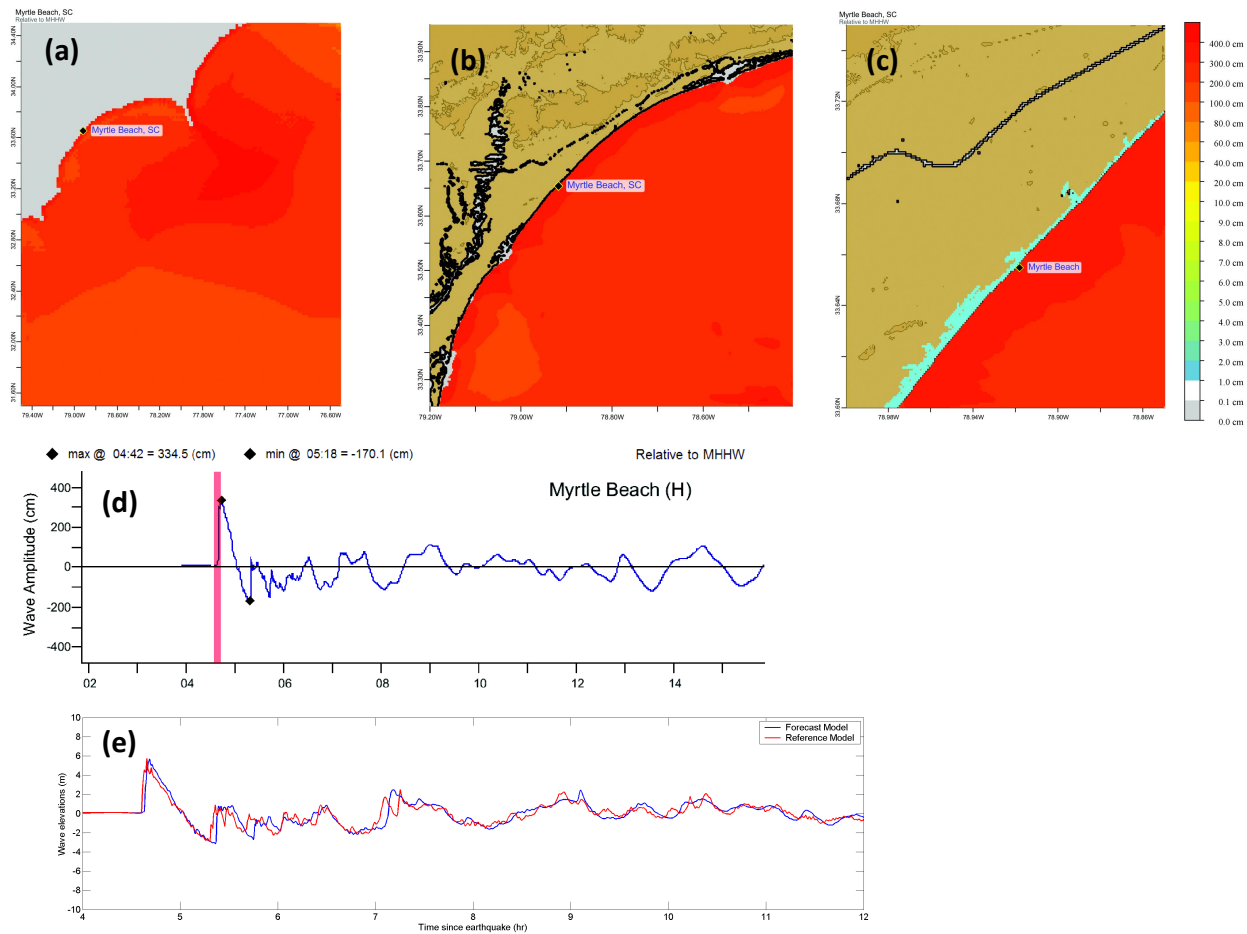
Figure C2: Response of the Myrtle Beach forecast model to synthetic scenario ATSZ 48-57 (α=25). Maximum sea surface elevation for (a) A-grid, b) B-grid, c) C-grid. Sea surface elevation time series at the C-grid warning point (d). The lower time series plot (e) is the result obtained during model development and is shown for comparison with test results.
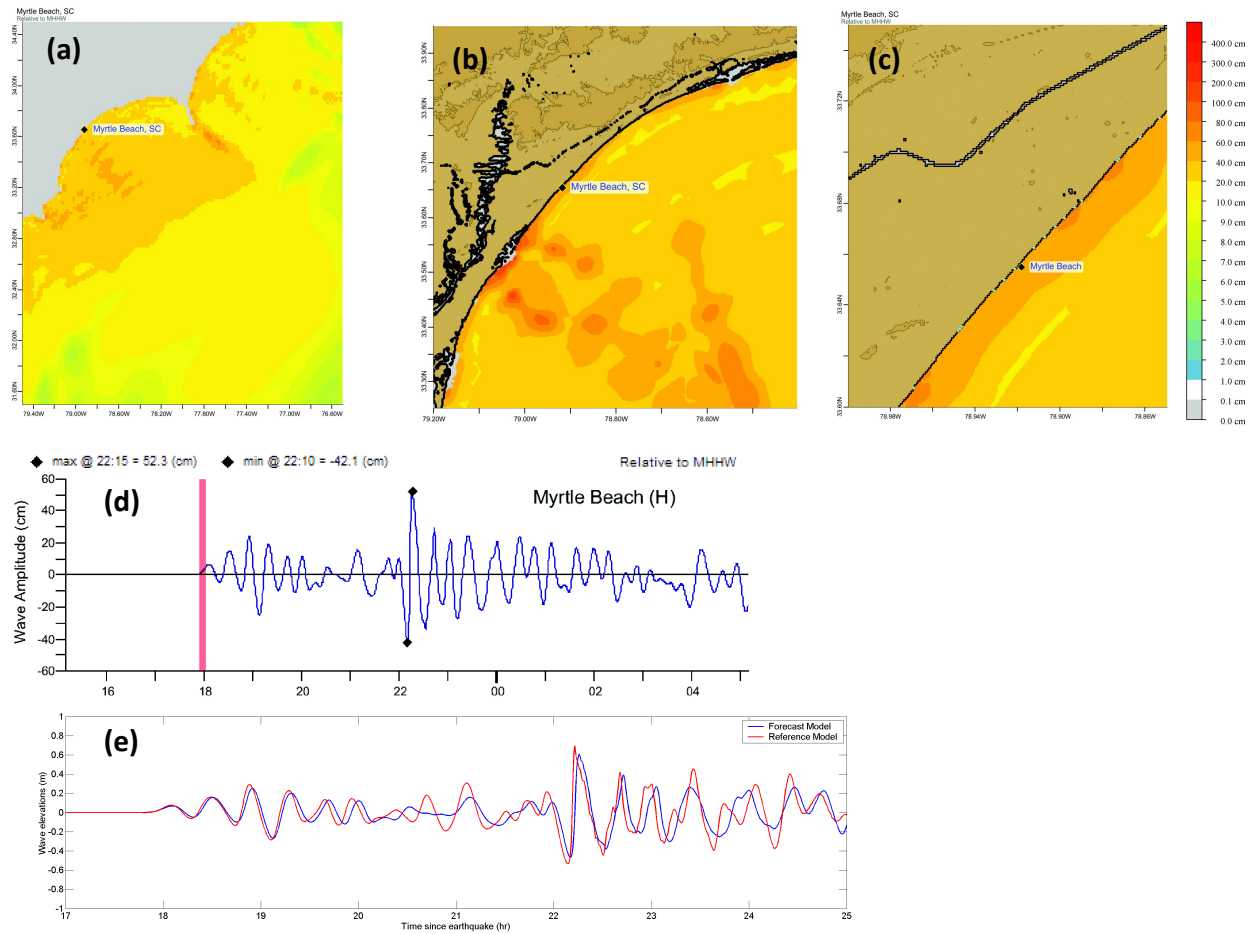
Figure C3: Response of the Myrtle Beach forecast model to synthetic scenario SSSZ 1-10 (α=25). Maximum sea surface elevation for (a) A-grid, b) B-grid, c) C-grid. Sea surface elevation time series at the C-grid warning point (d). The lower time series plot (e) is the result obtained during model development and is shown for comparison with test results.

Table C1: Run time of the Myrtle Beach, South Carolina forecast model.

Model	Modeled Time [hrs]	Wall Time [min]	4-hour Time [min]	Space [Gb]	12-hour Space [Gb]
LW2-atsz38-47.03b.IF_MYB	13.99	04.13	01.16	0.00	0.00
LW2-atsz48-57.03b.IF_MYB	13.99	04.13	01.16	0.00	0.00
LW2-sssz1-10.03a.IF_MYB	13.99	04.15	01.16	0.00	0.00

Table C2: Table of maximum and minimum amplitudes (cm) at the Myrtle Beach, South Carolina warning point for synthetic and historical events tested using SIFT 3.2 and obtained during development.

Scenario Name	Source Zone	Tsunami Source	α [m]	SIFT Max (cm)	Development Max (cm)	SIFT Min (cm)	Development Min (cm)
Mega-tsunami Scenarios							
ATSZ 38-47	Atlantic	A38-A47, B38-B47	25	126.9	123.5	-69.1	-69.1
ATSZ 48-57	Atlantic	A48-A57, B48-B57	25	334.5	335.0	-170.1	-170.0
SSSZ 1-10	South Sandwich	A1-A10, B1-B10	25	42.3	52.5	-42.1	-42.1